12-2010

Sequencing and functional analysis of a multi-component dioxygenase from PAH-degrading Sphingomonas paucimobilis EPA505

Renuka Miller
Clemson University, ren621@yahoo.com

SEQUENCING AND FUNCTIONAL ANALYSIS OF A MULTI-COMPONENT DIOXYGENASE FROM PAH-DEGRADING *SPHINGOMONAS PAUCIMOBILIS* EPA505

A Dissertation
Presented to
the Graduate School of
Clemson University

In Partial Fulfillment
of the Requirements for the Degree
Doctor of Philosophy
Microbiology

---

by
Renuka Persad Miller
December 2010

Accepted by:
Thomas A. Hughes, Committee Chair
Steven Hayasaka
Jeremy Tzeng
Annel Greene

ABSTRACT

Polycyclic aromatic hydrocarbons (PAHs) are hydrophobic organic compounds consisting of two or more fused benzene rings. PAHs derive from many different sources including petroleum refining, wood treatment, and coal coking industries. Because of their structural stability and water insolubility, PAHs are extremely resistant to degradation. These compounds are also believed to have mutagenic, carcinogenic, and teratogenic effects. Therefore, there are currently 16 PAH compounds on the EPA's list of priority pollutants.

Many species of bacteria have the ability to breakdown these persistent pollutants. However, bioremediation strategies using these organisms have many unresolved issues. While laboratory experiments can easily demonstrate the ability of these organisms to breakdown pollutants, environmental factors may reduce degradation abilities *in situ*.

Within the prokaryotes, members of the genus *Sphingomonas* have demonstrated a greater ability to breakdown PAHs. *Spingomonas paucimobilis* EPA505, for example, was shown to degrade a wide range of PAHs including the high molecular weight PAH fluoranthene, which it could also use as a sole carbon source. Because of its potential as a bioremediation tool, it is important to study the molecular basis of PAH catabolism in EPA505.

A genomic library of EPA505 was constructed and probed for genes involved in PAH degradation. Complete gene sequences were obtained for four subunits which are involved in the first step of the PAH catabolism. This step is catalyzed by a dioxygenase enzyme and yields a dihydrodiol intermediate. Two of the gene sequences encode an

alpha and beta subunit of the dioxygenase. The third gene encodes a ferredoxin subunit and the fourth gene codes for a ferredoxin reductase subunit.

The four genes were cloned for expression. Expression host cells were induced to test the activity of the four recombinant proteins on various PAHs. When cells expressing all four subunits were incubated with naphthalene and phenanthrene, the corresponding dihydrodiol product was detected using GC-MS. No dihydrodiol product was detected when fluoranthene was tested. In addition, no dihydrodiol products were detected for any substrate when cells lacking the two ferredoxin subunits were tested.

This study identified and showed functional analysis of one enzyme, a PAH degrading dioxygenase in the PAH catabolic pathway of *Sphingomonas paucimobilis* EPA505. There is still much to learn in order to fully appreciate and take advantage of this organism as an efficient tool for bioremediation.

DEDICATION

I dedicate this work to Robindra Persad, my loving father and devoted teacher, who has always been my greatest source of inspiration. His support and guidance has carried me through, from grade school to grad school.

ACKNOWLEDGMENTS

I would like to thank my advisor Dr. Thomas Hughes and my committee members, Dr. Steven Hayasaka, Dr. Jeremy Tzeng, and Dr. Annel Greene for all their help and support throughout my years at Clemson. I would also like to thank Dr. Harry Kurtz and Dr. Mike Henson for taking the time to help me whenever I needed their advice and expertise.

Thanks to Dr. Chris Saski and others at CUGI for their assistance with the genomic library construction and sequencing. I would also like to thank Dr. Melissa Riley and Fran Harper for their invaluable input with the enzyme activity assays and use of the analytical lab.

Thanks to John Abercrombie and Bode Olukole who have always been true and dependable friends and always made time to help with anything I needed. I would also like to thank my labmates and colleagues Aaron Brown, Jaleh Jalili, Sujay Guha, Hari Kotturi, Sara Garrett, Jyothi Rangenini and all other friends who have given me so much support and made grad school an enjoyable and unique experience.

Most importantly, I am grateful to my family including my husband Jay, my mother Audrey, my brother Shiva, my grandfather Lutchmee and my extended family for their love and patience throughout my many years in school.

TABLE OF CONTENTS

Page

LIST OF TABLES

LIST OF FIGURES

List of Figures (Continued)

Figure Page

LITERATURE REVIEW

1.1 Polycyclic Aromatic Hydrocarbons

Polycyclic aromatic hydrocarbons (PAHs) are hydrophobic organic compounds consisting of two or more fused benzene rings. Ring arrangement can be linear, angular or clustered. These compounds are generally classified into two categories based on size: 1) low molecular weight (LMW) PAHs which contain two or three benzene rings and 2) high molecular weight (HMW) PAHs which contain four or more rings. For example, naphthalene, phenanthrene and anthracene would be considered LMW PAHs whereas, fluoranthene, pyrene and chrysene would be considered HMW PAHs.

PAHs derive from many different sources including petroleum refining, wood treatment, and coal coking industries. Other sources of PAHs can include gasoline and diesel fuel combustion, and tobacco smoke (1). PAHs are ubiquitous pollutants which can contaminate water, vegetation and food. These compounds and their derivatives can be found in the air, soil, surface water, groundwater and runoff. Pollutant concentration varies widely throughout the environment ranging from 1µg/kg to over 300g/kg. Factors that determine the amount of contamination include distance from the source, level of industrial development, and mode of transport for the pollutant (39).

The aromatic structures of PAHs make them chemically stable molecules. They are water insoluble and form hydrophobic interactions with soil particles. Because of their structural stability and water insolubility, PAHs are extremely resistant to degradation. They sorb strongly to soil particles and become inaccessible for degradation. Larger

PAH molecules are more hydrophobic, and more resistant to degradation and therefore have a higher prevalence in the environment. For example, phenanthrene, a three-ringed PAH, may have a half life of 16 to 126 days. The half life of the five ringed PAH benzo[*a*]pyrene (B*a* P), however, can range from 229 to 1,400 days (3).

1.2 Health Risks

Health risks associated with PAHs have been well documented. These compounds are thought to have mutagenic, carcinogenic, and teratogenic effects. Because of these concerns, there are currently 16 PAH compounds on the EPA's list of priority pollutants (Table 1.1) (4).

Kusk et al. (5) found a significant decrease in the photosynthetic activity of green algae that were exposed to PAHs. PAHs have also caused digestive cell death in mussels (6), decreased reproductive rates in rainbow trout (7), and increased mortality rates in crustaceans (8).

With regard to mammalian studies, mice that were fed high levels of one PAH during pregnancy had difficulty reproducing as did their offspring. The offspring also had higher rates of birth defects and lower body weights (4). PAHs have caused lung cancer in laboratory animals that were exposed to contaminated air, stomach cancer when fed contaminated food, and skin cancer when PAHs were applied directly to the skin (4).

PAHs can contaminate vegetation through the soil and through runoff. They can then be taken up by mammals through the digestive tract when contaminated food is ingested (9). PAHs can even be transferred to humans through the consumption of seafood that

was caught in contaminated waters (10). Because of the chemical nature of these compounds, they might associate with lipid components in biological tissues and interact with DNA to cause mutations in both prokaryotic and eukaryotic cells (11).

An example of the toxic effects of PAHs can be shown with naphthalene. Naphthalene binds to molecules in the liver, kidney and lung tissues and is known to inhibit mitochondrial respiration (12). Phenanthrene, is known to be a photosensitizer of human skin and is also mutagenic to bacteria (13). These are examples of some of the effects of LMW PAHs and it is thought that larger PAHs pose more serious health hazards (14).

It is true that these pollutants do undergo degradation in the environment over time. The rate at which this occurs, however, is much slower than the rate at which new PAHs are released into the environment. The Exxon Valdez oil spill of 1989, for instance, affected the fate of many organisms. The pink salmon community in particular showed a reduction in egg survival rates for many years. Contaminants were also transferred by tidal cycling and hydraulic gradients to reach developing embryos. In recent years, significant changes in the spawning habitats were seen, which indicated the salmon were recovering from the spill (15). Although this is good news, it is evidence of the persistence of PAHs in our environment. After more than a decade, the effects of this major environmental incident have still not completely disappeared.

Old PAH contamination is not the only problem to solve. There are much more recent examples of large scale PAH pollution. The September 11th attacks gave rise to the release of 100-1000 tons of PAHs throughout lower Manhattan and beyond. The highest

PAH concentrations were found at the sites closest to the fires. Those involved in the cleanup have been affected greatly. There have been numerous reports of PAH related respiratory illness including, persistent coughs, bronchitis, and new cases of asthma. It is said that these people and others who were exposed have a real risk for lung cancer in the future (16).

1.3 Bioremediation

Many bioremediation strategies have been developed to clean up PAH contamination. Some species of bacteria, fungi and even plants have the ability to degrade these pollutants.

Although it was believed that eukaryotic organisms could not cleave the fused rings of PAHs, Hammel et al. showed the mineralization of phenanthrene by the lignolytic fungus *Phanerochaete chrysosporium* (17). The white rot fungus *Pleurotus ostreatus* also demonstrated the ability to metabolize phenanthrene (18).

Phytoremediation, another bioremediation strategy, involves the use of plants to clean up contaminated soil. Levels of acenaphthalene, anthracene, phenanthrene, naphthalene, and fluoranthene all decreased significantly in soils planted with green ash and hybrid poplar trees compared to unplanted soils. There was also an increase in the population of microbial degraders in the planted soil versus the unplanted soil (3). The authors suggested the trees increased the rates of PAH degradation through microbial activity in the rhizosphere.

Although bacteria in the rhizosphere might assist plants in effectively degrading PAHs, they can certainly clean up contaminated soils independently. Bacteria are well known for their adaptation abilities and diverse characteristics. Many species of bacteria are known to degrade PAHs. Heitkamp and Cerniglia found *Mycobacterium* PYR-1 can degrade fluoranthene, naphthalene and phenanthrene but cannot use these compounds as a sole carbon source (19). Analysis of contaminated soil samples led to the identification of three strains of PAH degrading *Burkholderia cepacia*. All three isolates degraded fluorene, phenanthrene, pyrene, fluoranthene, benz[*a*,*h*]anthracene, dibenz[*a*,*h*]anthracene and benzo[*a*]pyrene (20). Krivobok et al. (2) showed ^{14}C-pyrene mineralization by *Mycobacterium* sp. strain 6PYI. An increase in catabolic activity and the expression of two ring-cleavage proteins was observed in cells grown on pyrene compared to those grown on acetate (2). *Alcaligenes denitrificans* strain WW1 was isolated by Weissenfels et al. (21) and was found to degrade fluoranthene at a rate of 0.3 mg/ml a day. Other PAHs, including pyrene and benz[*a*]anthracene were also degraded by strain WW1 via cometabolic processes (21). *Cycloclasticus*, an organism isolated from marine sediments was able to partially degrade 1 ppm pyrene and 1 ppm fluoranthene when 10 ppm phenanthrene was provided in culture (10). While these findings are important, few organisms have been found which can degrade compounds with more than three fused benzene rings and additionally can use these compounds as sole sources of carbon and energy.

1.4 Problems with Bioremediation

Although bacteria can breakdown PAHs, this does not mean the PAH pollution problem is solved. In fact, bioremediation through the use of PAH degrading bacteria like EPA505 has great potential for PAH cleanup, but there are many unresolved problems. While laboratory experiments can easily demonstrate the ability of these organisms to breakdown pollutants, environmental factors may reduce degradation abilities *in situ*. Some of the factors that affect the efficiency of *in situ* degradation include targeting microbes to the pollutants, soil moisture, oxygen, temperature, pH, microbial predation, availability of nutrients, and the production of inhibiting metabolites**.**

One major problem with bioremediation has to do with the chemical nature of PAHs. Because of hydrophobic interactions, PAHs are sometimes inaccessible to microbial degraders in the environment. Whereas smaller organic compounds might be degraded, large PAH molecules are tightly bound to soil particles and as a result accumulate (22).

Another problem with bioremediation of PAHs is partial degradation. Some organisms can begin to breakdown the initial compound, but environmental factors may inhibit the complete breakdown process. Partial degradation of PAHs can pose a bigger threat as metabolites may be more toxic than parent compounds. Bouchez et al. (4) studied the co-metabolic activity of six bacterial strains grown on several different PAHs. Synergistic activity as well as inhibition was noted. Furthermore, the production of water soluble metabolites was found consistently throughout the experiment (4).

If inhibition leads to the accumulation of water soluble intermediate metabolites, the result might be contaminated water sources.

Some PAHs are partially broken down through abiotic processes such as photooxidation. While this may seem helpful, it can actually lead to a bigger problem. Phenanthrene for example, can be converted by sunlight to the more polar product 9,10-phenanthrenequinone (PheQ). PheQ can react with biomolecules and, therefore, is much more toxic than its parent compound phenanthrene. The increased toxicity of PheQ compared to phenanthrene was demonstrated in bacteria (23) and plants (24). PheQ was also shown to inhibit naphthalene degradation by *Burkholderia*. There was a 20% degradation of naphthalene in the presence of PheQ as compared to a 75% degradation with no PheQ. The same study showed that a *Sphingomonas* species could degrade PheQ, but only in the presence of phenanthrene (25).

Bioremediation problems also exist with *S. paucimobilis* EPA505. For example, fluoranthene degradation by EPA505 is sometimes inhibited by creosote constitutents. An experiment was done to determine which creosote components were actually inhibiting the breakdown process. Creosote compounds were categorized into three groups: acidic (phenolics), basic (N-heterocyclics), and neutral (PAHs). Results indicated the inhibitory effects were mostly a result of the basic components in creosote (26). Although the authors found the chemical source of the problem, they did not know why there was inhibition. More information on gene expression and regulation might lead to solutions to these types of problems.

1.5 Sphingomonads

The Sphingomonads refer to organisms belonging to one of four genera including: *Sphingomonas*, *Sphingobium*, *Sphingopyxis*, and *Novosphingobium*. Members of this group are widespread in the environment. They have been isolated from both aqueous and terrestrial habitats as well as clinical specimens and other sources (27).

First described by Yabuuchi et al. (1990), the Sphingomonads are Gram-negative, chemoheterotrophic, non-spore forming rod-shaped bacteria. These organisms typically produce yellow pigmented colonies. Some cells may contain a single polar flagellum, but others may be non-motile. One distinctive characteristic of these organisms is that they have glycosphingolipids in their cell envelopes instead of the more typical lipopolysaccharides (27). Although there is no evidence to date, it has been suggested that these glycosphingolipids may play a role in the successful uptake of PAHs for biodegradation (28).

Representatives of the genus *Sphingomonas* seem to have a wider range of substrates than other organisms. For example, *Novosphingobium aromaticivorans* strain F199 can grown on toluene, xylene, *p*-cresol, biphenyl, naphthalene, dibenzothiophene, fluorene, salicylate and benzoate (29,30). *S. yanoikuyae* B1 can grown on 1,2,3- trimethylbenzene, toluene, p-xylene, biphenyl, naphthalene, phenanthrene and anthracene (31).

In addition to a wider range of substrates, certain Sphingomonad species can utilize PAHs as a sole carbon and energy source. For example, whereas many other organisms have been shown to degrade two and three-ringed PAHs such as naphthalene,

phenanthrene and anthracene, the Sphingomonads can also break down HMW PAHs with four and five-rings such as fluoranthene, pyrene, and benzopyrene (32).

Sphingomonas paucimobilis EPA505 was isolated from a seven member community from a creosote waste site (33). It was one of the first organisms reported to degrade and use a HMW PAH (fluoranthene) as a sole carbon and energy source (34). Fluoranthene utilization was shown by an increase in cell biomass, disappearance of the HMW PAH, and by the production of metabolites. Additionally, EPA505 cells grown on fluoranthene could degrade other compounds such as benzo[*b*]fluorene, benz[*a*]anthracene, chrysene, and pyrene (34). Ye et al. (1) studied the degradation activity of fluoranthene grown EPA505 cells on other HMW PAHs. After 16 hours of incubation with 10 ppm of the specific compound, *S. paucimobilis* degraded 80% of pyrene, 72.9% benz[*a*]anthracene, 31.5% chrysene, 33.3% benzo[*a*]pyrene, 12.5% benzo[*b*]fluoranthene, and 7.8% dibenz[*a,h*]anthracene. They also found an increase in degradation activity with increased cell density. In addition, cells that were incubated with [7-^{14}C] labeled benzo[*a*]pyrene, and [5, 6, 11, 12-^{14}C] labeled chrysene for 48 hours, degraded 28% of the former and 42% of the latter to $^{14}CO_2$ (1).

1.6 PAH Catabolic Pathway

Naphthalene is commonly used as a model compound for PAH degradation studies. Although there are some exceptions, the primary pathway for naphthalene degradation is divided into an upper and lower catabolic pathway. For the upper catabolic pathway, (Fig. 1.1) the first step occurs when a ring hydroxylating dioxygenase introduces two

molecules of oxygen to initiate cleavage of the aromatic ring and form naphthalene *cis*-dihydrodiol. The dihydrodiol product is then dehydrogenated to 1,2-dihydroxynaphthalene by a *cis*-naphthalene dihydrodiol dehydrogenase. The next step involves another dioxygenase, namely 1,2-dihydroxynaphthalene dioxygenase which yields the product 2-hydroxy-2H-chromene-2-carboxylic acid. The next two reactions are catalyzed by a carboxylate isomerase and a hydratase-aldolase to give salicylaldehyde. This product is converted to salicylate by a dehydrogenase. In the lower catabolic pathway (Fig. 1.2) salicylate is further degraded to TCA cycle intermediates either through the catechol or gentisate pathways. Similar catabolic steps are involved for the degradation of phenanthrene, anthracene and other aromatic hydrocarbons.

1.7 Genetics of PAH Degradation in Sphingomonads

The genetics of PAH degradation have been studied in some *Sphingomonas* species. The genes involved in aromatic hydrocarbon degradation in this group seem to be highly conserved and have been shown to be different from those described in other genera (28).

The sequence of a 40kb region from *Sphingobium yanoikuyae* B1 revealed over 35 genes on 6 different operons involved in aromatic hydrocarbon degradation. While at least five sets of ring-hydroxylating dioxygenases were found, only one ferredoxin reductase (*bphA4*) and ferredoxin (*bphA3*) was found among all the genes identified. However, these two proteins were found to be associated with multiple dioxygenase components (35). Analysis of the genes in B1 also revealed that the first three enzymes in the pathway work on a broad range of substrates and can metabolize naphthalene,

phenanthrene and biphenyl. The *nahD* gene of B1 encoding the 2-hydroxychromene-2-carboxylate isomerase, however, was only involved in the degradation of naphthalene (35). *Sphingobium yanoikuyae* B1 is unusual in that the genes required for the degradation of a compound are not arranged on the same operon (28).

The complete sequence of a 184-kb catabolic plasmid, pNL1, from *Novosphingobium aromaticivorans* strain F199 has been ascertained (36). Romine et al. found 79 genes on the plasmid that are associated with breakdown or transport of PAHs. Of the genes identified, those that are involved in PAH degradation are in the same order and transcriptional direction as the same genes on strain B1. In addition to the five dioxygenase components found in B1, a sixth terminal oxygenase component was identified on pNL1 (36). Genes *xylB, nahF, bphD, bphE* and *bphF* were also identified on pNL1, but functional analysis has not yet been done (28).

In *Sphingobium* strain P1, transposon mutagenesis interrupted the ferredoxin subunit (*ahdA4*) of a dioxygenase, impairing the ability of the organism to degrade phenanthrene. As with strain B1, five sets of terminal oxygenase components were also identified, but only one ferredoxin and one ferredoxin reductase were identified. Additionally, two meta-cleavage enzymes *bphC* and *xylE* were identified which had 100% identity with those genes of strain B1 (37).

Recently, the sequence of an aromatic ring-hydroxylating dioxygenases of *Sphingomonas* strain CHY-1 were identified and tested for enzymatic activity. Demaneche et al. found the sequence of two genes coding for the alpha and beta subunits of a terminal oxygenase, *phnA1a* and *phnA2a* (38). The product of these two genes was

collectively called PhnI. Genes encoding a ferredoxin component (*phnA3*) and ferredoxin reductase component (*phnA4*) were also identified on separate loci. All four genes were highly similar to genes found in strain F199. When incubated with several different substrates, recombinant PhnI converted PAHs to the respective dihydrodiol products. Furthermore, enzyme activity increased greatly with the co-expression of the ferredoxin and ferredoxin reductase subunits (38).

Limited work has been done on the genetics of PAH degradation in *Sphingomonas paucimobilis* EPA505. Tn5 mutants were used to delineate the catabolic pathway of EPA505. Story et al. also found that while a common hydroxylase is involved in the pathways for the different substrates studied, EPA505 possesses two distinct hydratase-aldolase genes. One is involved in the degradation of naphthalene, phenanthrene and anthracene, and the other involved in fluoranthene degradation (40). It was suggested that the genes involved in PAH degradation in strain EPA505 are located on several different operons as seen in the other members of this group.

Partial gene sequences were obtained for some of the genes involved in the PAH catabolic pathway of EPA505 when the regions flanking Tn5 inserts were sequenced. Because of its wide range of substrates and ability to grow on some compounds as a sole source of carbon, *S. paucimobilis* EPA505 has great potential for bioremediation. It is therefore necessary to study the genetic basis of degradation in this organism in more detail.

1.8 Ring-Cleaving Dioxygenases

As mentioned earlier, there are several enzymes involved in the PAH upper catabolic pathway (Fig 1.1). The first enzyme in the pathway is a ring-hydroxylating dioxygenase. This enzyme initiates the breakdown of the PAH substrate by introducing two oxygen molecules into the aromatic ring structure to form a dihydrodiol product.

These enzymes are all soluble, multi-component systems that are usually made up of two or three separate proteins including: a ferredoxin, a ferredoxin reductase and an iron-sulfur protein. The iron-sulfur protein is made up of an alpha and beta subunit and is the catalytic oxygenase component (41). The proteins are arranged in a short electron-transport chain where electrons are moved to the catalytic terminal oxygenase (Fig. 1.3) (28).

For naphthalene dioxygenase, the reductase component is the first component in the electron-transport chain. Transport is initiated by a single two-electron transfer from NAD(P)H to FAD in the ferredoxin reductase which gives the reduced form of FAD. The reduced FAD then provides electrons to the ferredoxin. These electrons are then transferred to the iron-sulfur protein or terminal oxygenase which uses the electrons in its active site to introduce an oxygen molecule into the aromatic ring (28). The terminal oxygenase component of the chain consists of three alpha and three beta subunits. These subunits come together to form a mushroom like shape with the three alpha subunits forming the cap and the three beta subunits forming the stem (52).

The substrate specificity of naphthalene dioxygenase has also been investigated. Parales et al. showed that the Asp-205 residue in the catalytic domain of naphthalene

dioxygenase is necessary for activity. When site-directed mutagenesis was employed to change this residue to either, alanine, glutamate, asparagine or glutamine, mutant proteins were not able to transform naphthalene to the dihydrodiol product. In addition, oxygen uptake by the mutant protein was decrease when compared to the wild-type (42). This study confirmed that aspartate was responsible for the successful transfer of electrons to the active site.

Although *S. paucimobilis* EPA505 has the ability to break down a wide range of substrates and exhibits greater PAH degrading capabilities when compared to other organisms, there is limited information on the catabolic enzymes in this organism. The purpose of this work was to identify complete gene sequences encoding PAH degrading dioxygenases in EPA505, compare the sequences identified to those in related organisms, and carry out functional analysis of the enzymes. Fundamental knowledge of PAH-catabolic genes and gene products in this strain may ultimately give way to more efficient bioremediation strategies.

Table 1.1 US EPA's 16 priority-pollutant PAHs and selected physical–chemical properties.

PAH	Chemical Structure	Molecular weight g/mole	Solubility mg/L
Naphthalene		128.17	31
Anthracene	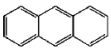	178.23	0.045
Phenanthrene		178.23	1.1
Pyrene	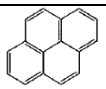	202.26	0.132
Acenaphthene		154.21	3.8
Acenaphthylene		152.20	16.1
Flourene	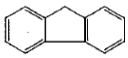	166.22	1.9
Fluoranthene	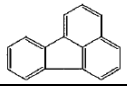	202.26	0.26
Chrysene	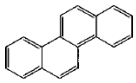	228.29	0.0015
Benzo (a) pyrene	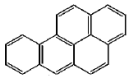	252.32	0.0038
Benz (a) anthracene	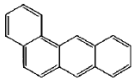	228.29	0.011
Benzo (k) fluoranthene	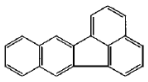	252.32	0.0008
Indeno (1,2,3- cd) pyrene	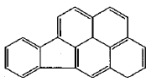	276.34	0.062
Benzo (b) fluoranthene	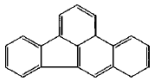	252.32	0.0015
Dibenzo (a,h) anthracene	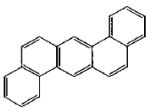	278.35	0.0005
Benzo (g,h,i) perylene	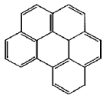	276.34	0.00026

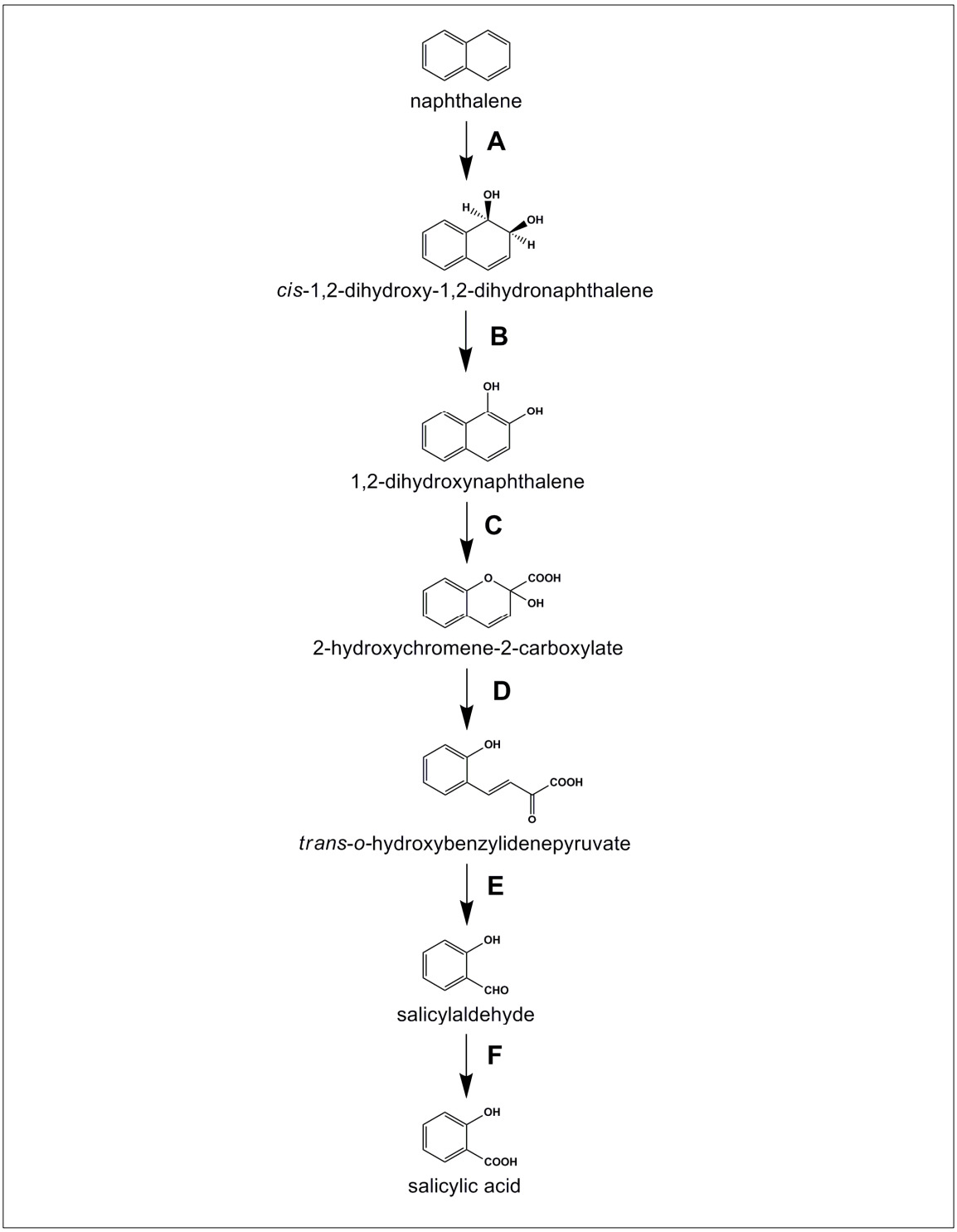

Figure 1.1 Upper catabolic pathway of naphthalene degradation (60). Enzymes: (A) naphthalene dioxygenase, (B) *cis*-naphthalene dihydrodiol dehydrogenase, (C) 1,2-dihydroxynaphthalene dioxygenase, (D) 2-hydroxychromene-2-carboxylate isomerase, (E) *trans*-*o*-hydroxybenzylidenepyruvate hydratase-aldolase, (F) salicylaldehyde dehydrogenase.

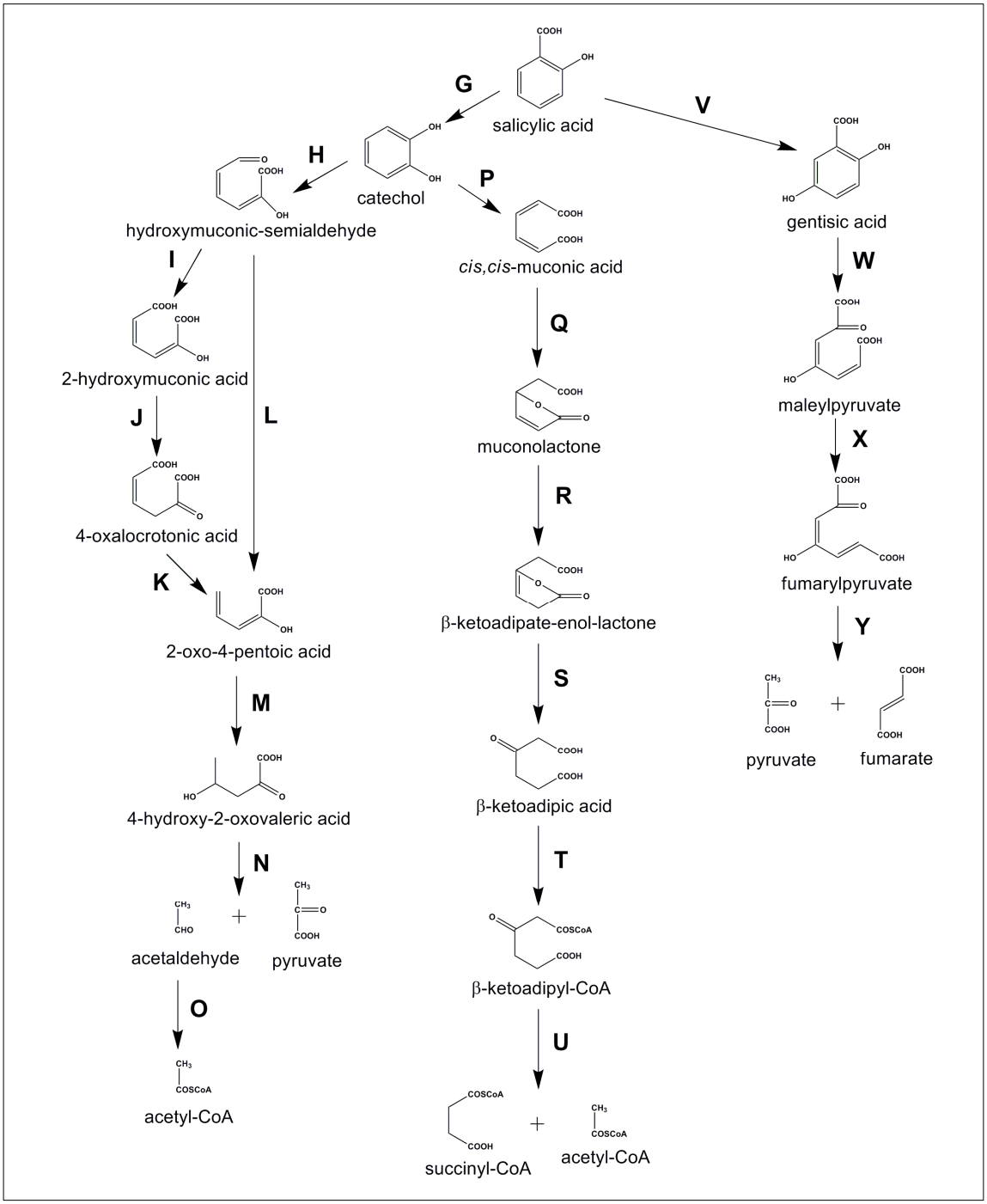

Figure 1.2 Naphthalene lower catabolic pathway. Salicylic acid created in the upper pathway is further metabolized either through the catechol or gentisic acid pathways to TCA cycle intermediates (60).

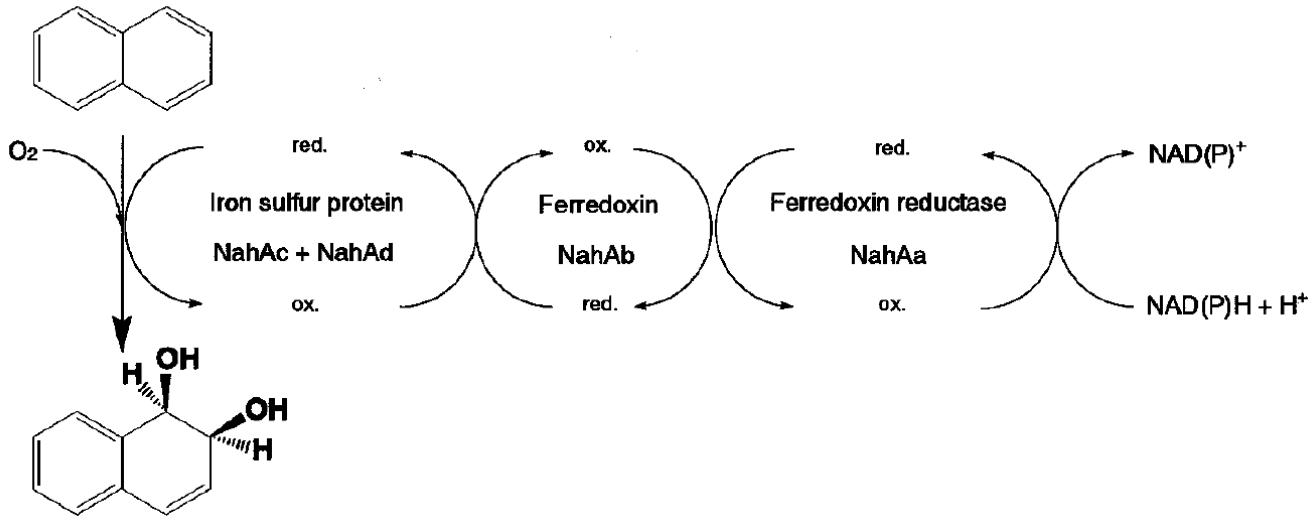

Figure 1.3 Initial step of naphthalene oxidation catalyzed by a multi-component dioxygenase (28). The ferredoxin reductase accepts electrons and transfers them to a ferredoxin which transfers again to the terminal oxygenase components. The reduced terminal oxyenase then catalyzes the oxidation of the aromatic compound to produce a dihydrodiol (41).

MATERIALS AND METHODS

2.1 Reagents

All PAHs, solvents, antibiotics, and derivatizing agents were purchased from Sigma-Aldrich (St. Louis, MO). Primers and oligonucleotides were purchased from Integrated DNA Technologies (San Diego, CA). Unless otherwise stated, restriction endonucleases and other DNA modification enzymes were purchased from Promega (Madison, WI).

2.2 Bacterial Strains, Plasmids and Growth Conditions

Sphingomonas paucimobilis EPA505 was isolated from a creosote waste site (34). One colony of *S. paucimobilis* EPA505 was inoculated into 10 ml of Luria Bertani (LB) broth and incubated at 37°C with shaking. When the culture reached late log phase, chloramphenicol was added to a final concentration of 200 µg/ml and the culture was incubated further at 37°C with shaking for one hour. Chloramphenicol was added to ensure the genomic DNA collected was from cells in late log phase. After treatment with chloramphenicol, cells were harvested and prepared for library construction.

E. coli strains and plasmids used are listed in Table 2.1. All organisms for recombinant DNA experiments were grown in LB media supplemented with the appropriate antibiotics.

2.3 BAC Library Construction

Genomic library construction was carried out at the Clemson University Genomics Institute (CUGI). To construct a BAC (Bacterial Artificial Chromosome) library, high molecular weight (HMW) bacterial DNA was first embedded into agarose plugs. *S. paucimobilis* EPA505 cells were harvested from a late exponential phase culture and washed once with 2 ml of NaCl/Tris(pH7.2)/EDTA (200mM NaCl, 10 mM Tris-Cl, 100mM EDTA)and then resuspended in 0.5 ml of the same buffer. The cell suspension was then placed in a 37°C water bath for 5 minutes. A solution of 2% (w/v) SeaPlaque GTG agarose (FMC BioProducts, Rockland, ME) in water was prepared and equilibrated to 40°C in a water bath. One volume of the agarose solution was mixed with the cell suspension, mixed and the solution was poured into plug molds. After setting, the plugs were removed and placed in a 15 ml screwcap tube and 2-3 volumes of bacterial cell lysis solution for HMW DNA (10 mM Tris-Cl, 50 mM NaCl, 100 mM EDTA, 0.2% sodium deoxycholate, 0.5% *N*-lauroylsarcosine, 1mg/ml lysozyme) was added and the mixture incubated at 37°C for 2-16 hours. All BAC library construction procedures after preparation of genomic DNA were carried out as previously described (53).

2.4 Overgo Probing of High-Density BAC Membranes

Following BAC library construction, high density membranes were made in order to probe the library for genes of interest. Overgo probes were designed from partial PAH gene sequences previously obtained from EPA505 (40). To carry out hybridization, 50 ml of warm hybridization solution (1% BSA, 1 mM EDTA, 7% SDS, 0.5 M sodium

phosphate) was added to a hybridization bottle. Membranes were pre-moistened with warmed 2X SSC and then rolled into a hybridization bottle for a 4-hour prehybridization. After prehybridization, about 10 ml of hybridization buffer was removed from the bottle. After denaturing the labeled overgos at 90°C for 10 minutes, the probes were added to the 10ml of buffer and mixed. The 10 ml was then added back to the bottle with the membrane. Probes were allowed to hybridize overnight in a hybridization oven set at 60°C with rotation.

After hybridization, the buffer was removed and the membrane was washed three times. The membrane was washed first with 1x SSC, 0.1% SDS, second with 1.5x SSC, 0.1% SDS and once more with 0.75X SSC, 0.1% SDS. All three washes were carried out at 58°C for 30 minutes. For autoradiography, the filter was sealed in a plastic zip top bag and exposed to XAR5 film at 70°C.

2.5 Southern Analysis

BAC clones containing genes of interest were digested and analyzed by Southern blot/hybridization. BAC DNA was purified by maxi-prep (43). Purified DNA was then digested at 37°C overnight with HindIII and BamHI (Promega, Madison, WI) and size fractionated in a 0.8% (w/v) SeaKem LE agarose gel (BioWhittaker Molecular Applications, Rockland, ME) using 1× TAE (40 mM Tris-acetate, 1 mM EDTA, pH 8.0) as a running buffer.

After separation was completed, the gel was depurinated by incubation in 0.125 N HCl followed by a 30 minute incubation in denaturing buffer (1.5 M NaCl, 0.5 M

NaOH), and finally a 30 minute incubation in neutralization buffer (1.5 M NaCl, 0.5 M Tris pH 7.5). DNA was transferred to Hybond-XL membrane (Amersham Pharmacia Biotech, Little Chalfort, Buckinghamshire, England) by capillary blot using 10× SSC (pH 7) as a transfer buffer. Following transfer, DNA was fixed to the membrane by baking at 80°C for 2 hours.

The membrane was prehybridized at 65°C with a 0.5 M sodium phosphate, 7% sodium dodecylsulfate (SDS) hybridization buffer for a minimum of 30 minutes. Radioactively labeled and denatured DNA probe was added directly to the prehybridization solution, and the membrane was hybridized with the probe overnight at 65°C. The hybridized membrane was washed at 65°C twice with 2× SSC (pH 7.0), 1% (w/v) SDS for 30 minutes, and twice with 1× SSC, 0.1% (w/v) SDS for 30 minutes. The membrane was then exposed to autoradiographic film (Kodak X-Omat Blue XB-1, Perkin-Elmer Life Sciences, Inc., Boston, MA) overnight.

2.6 Shotgun Library Construction

To construct a shotgun library, BAC DNA was purified by maxi-prep (43) and subjected to random fragmentation by hydroshearing (Gene Machines, San Carlo, CA). Fragments between 3-5 kb were selected by agarose gel electrophoresis, subjected to end-repair/phosphorylation using the End-it end repair kit (Epicentre, Madison, WI), and was then cloned into the high copy plasmid pBlueskriptIIKSII+. Plasmids were then electroporated into *E. coli* DH10B cells. Transformants were selected on LB plates containing carbenicillin, X-Gal and IPTG. White recombinant colonies were picked

robotically using the Genetix Q-bot (Genetix, San Jose, CA) and stored as individual clones in Genetix 96-well microtiter plates as glycerol stocks at -80°C.

2.7 Primer Design

Primer3 software (47) was used to design primers (http://frodo.wi.mit.edu/primer3). Genes *phnA1a*, *phnA2a*, and *phnA3* were found on contigs assembled from high throughput sequencing. To clone these genes, primers were designed to include the appropriate restriction sites before and after the start and stop codons of the gene sequences. To locate *phnA4*, a series of primers were designed based on conserved regions of this gene. Several consecutive rounds of PCR using primer walking and 04N04 BAC DNA as a template were carried out to eventually obtain the entire *phnA4* gene.

2.8 Sequencing and Analysis

Sequencing was carried out at CUGI. Shotgun clones were sequenced using the universal priming sites on the vector. The data was collected on an ABI 3730xl DNA Analyzer (Applied Biosystems, Carlsbad, CA). For sequencing, 10 ng of DNA for every 1 kb of sequence and 0.3 µl of 2 µM primer were used.

DNA sequence and assembly was carried out using Phred, Phrap, and Consed (44). Sequence data was also assembled using Sequencher DNA assembly software (Gene Codes Corp, Ann Arbor, MI) and the free BioEdit sequence alignment editor program (mbio.ncsu.edu/BioEdit/bioedit.html). The GenBank tool BLAST at the NCBI server

was used to perform similarity searches for genes and proteins (48). GeneMark free gene prediction software (49) was used to search for open reading frames (exon.biology.gatech.edu). The ProtParam tool at the Expasy Proteomics Server (expasy.org/sprot) was used to determine the size, amino acid sequence and other properties of recombinant proteins. Phylogenetic trees were constructed using MEGA software version 4.0 (50) and multiple sequence alignments were carried out with ClustalW (51).

2.9 Cloning for Protein Expression

For protein expression, genes were cloned into the petDUET-1 and pACYCduet-1 vectors (Novagen, Madison, WI). Genes of interest were amplified using 04NO4 BAC DNA as a template and KOD Hot Start Polymerase according to the manufacturer's cycling recommendations (Novagen, Madison, WI). All PCR and gel purification steps were carried out using the Wizard SV Gel and PCR Clean-Up System (Promega Madison, WI).

Compatible Duet expression vectors were kindly provided by Dr. Michael Sehorn of Clemson University, Department of Genetics and Biochemistry (Fig. 2.1 and 2.2). Both Duet vectors were provided on agar plates within cultures of *E.coli* DH5α. Cells were grown overnight in LB broth supplemented with either ampicilin for pETDuet-1 (50µg/ml) or chloramphenicol for pACYCDuet-1 (34µg/ml). Plasmid extraction was carried out with Qiagen tip-100 and the midi-prep protocol (Qiagen, Valencia, CA).

PCR products were then digested as follows: *phnA1a* and *phnA3* PCR products were digested with BamHI and HindIII and were subsequently cloned into the BamHI and HindIII sites of petDUET-1 and pACYCduet-1, respectively. The *phnA2a* and *phnA4* PCR products were digested with BglII and KpnI and cloned into the second multiple cloning sites of petDUET-1 and pACYCduet-1, respectively. Digested vector was dephosphorylated with Thermosensitive Alkaline Phosphatase (Promega, Madison, WI). Ligation was carried out with the Ligafast Rapid DNA ligation system (Promega, Madison, WI). Genes *phnA1a* and *phnA2a* encoding two oxygenase components were cloned into pETDuet-1 to give pD12. Genes *phnA3* and *phnA4* encoding the ferredoxin and ferredoxin reductase components were cloned into pACYCDuet-1 to yield the plasmid pACD34.

Transformation was carried out according to the manufacturer's instructions into either *E. coli* Novablue host cells (Novagen, Madison, WI) for maintenance stocks, or into *E.coli* BL21(DE3) cells for expression of target proteins. Successful transformation and cloning were confirmed with colony PCR using vector specific primers.

2.10 Protein Expression/ SDS-PAGE

To express target proteins, BL21(DE3) cells were transformed with either pD12 or pACD34 or co-transformed with both plasmids to express all four proteins. Controls were also analyzed in which BL21(DE3) cells were transformed with the original vectors pETDuet-1 and/or pACYCDuet-1 containing no insert. LB broth plus the appropriate antibiotic was inoculated with one colony from the BL21(DE3) transformation and

incubated overnight at 37°C with shaking. The overnight culture was used to inoculate a secondary culture which was incubated at 37°C with shaking until the $OD_{600} > 0.5$. At this point the culture was split in half and IPTG was added to one half at a final concentration of 1 mM. The other half was not induced for comparison. The induced and uninduced cultures were returned to a 37°C incubator with shaking for up to 8 hours to analyze protein expression.

For SDS-PAGE analysis, cells were harvested and resuspended in phosphate buffered saline and 2x SDS loading dye (1:1). The suspension was then boiled for 5 minutes and centrifuged for 1 minute. Samples were then loaded onto tris-glycine precast gels (Biorad, Hercules, CA) with Smart Protein Middle-Range Standard protein marker (Genscript, Piscataway, NJ), and run at 120V until the dye front reached the bottom of the gel. Gels were visualized with Commassie blue staining (43).

2.11 Assay for Recombinant Protein Activity

BL21(DE3)(pD12) expressing the two oxygenase components and BL21(DE3)(pD12)(pACD34) expressing two oxygenase and two ferredoxin components were tested for enzyme activity. BL21(DE3)(pETDUET-1) and BL21(DE3)(pETDuet-1(pACYCDuet-1) harboring the plasmids without inserts were used as controls. Cells were grown in LB broth with appropriate antibiotics to an $OD_{600} > 0.5$.
IPTG was then added to a final concentration of 1mM and the culture was incubated at 25°C overnight with shaking. Cells were harvested and resuspended in M9 minimal medium plus 0.2% glucose at half the original volume so as to double the density of cells

in suspension. In addition, 100 µg of either: naphthalene, phenanthrene or fluoranthene dissolved in acetone was added to the cells. The culture was again incubated at 25°C with shaking overnight. After exposure to the PAHs, cells were harvested and the supernatant collected. The supernatant was extracted twice with ethyl acetate (1:1) and dried over sodium sulfate. Extracts were evaporated using a rotary evaporator and the residue was resuspended in 500 µl acetonitrile. Derivatization was carried out by combining 100 µl of the final acetonitrile suspension with 50 µl BSTFA:TMS (99:1) and incubated at 65°C for one hour to yield trimethylsilylated products. Samples were then analyzed by GC-MS. All experiments were done in triplicate. PAH standards dissolved in acetone were run for all substrates tested.

2.12 GC-MS analysis

Gas chromatography-mass spectrometry (GC-MS) was performed on an Agilent 7890 GC and an Agilent 5975 mass spectrometer with triple axis detector (Agilent, Santa Clara, CA). A J&W DB-5ms capillary column (30m by 0.25mm, 0.25µm film thickness) was used for separation of metabolites. GC-MS analyses were performed as follows: the initial oven temperature was set at 80°C and held for two minutes, the temperature was then increased at a rate of 8°C per minute until 300°C where it was held for 5 minutes. Electron ionization was achieved at 70eV electron energy and 150°C ion source temperature. Sample injection volumes were 2 µl splitless. Samples were run in scanning mode and the total run time was 34.5 minutes. Products were identified by

comparing the data collected to published mass spectra of specific dihydrodiol intermediates.

Table 2.1 List of bacterial strains and plasmids used in this study.

Bacterial strain or plasmid	Relevance/Properties	Source/Reference
Strains		
Sphingomonas paucimobilis EPA505	PAH degrading strain	Mueller et al., 1990
Escherichia coli DH10B	genomic library host	CUGI
Escherichia coli Novablue	maintenance host for cloned genes	Novagen
Escherichia coli BL21(DE3)	expression host	Novagen
Plasmids		
pCUGIBAC1	BAC library vector, Cam^r	CUGI
pBlueskriptIIKSII+	shotgun library vector, Amp^r	CUGI
pETDuet-1	protein expression vector, Amp^r	Novagen
pACYCDuet-1	protein expression vector, Cam^r	Novagen
pD12	pETDuet-1 with *phnA1a*, *phnA2a*	This study
pACD3	pACYCDuet-1 with *phnA3*	This study
pACD34	pACYCDuet-1 with *phnA3*, *phnA4*	This study

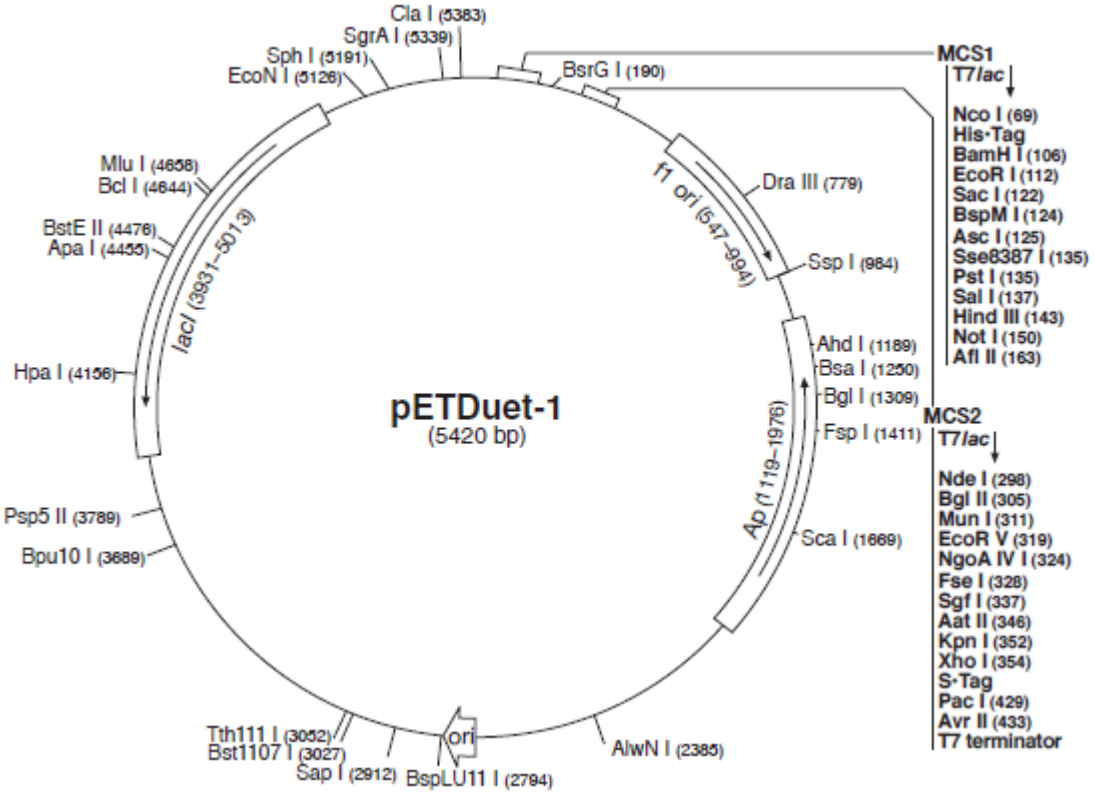

Figure 2.1 Vector map of pETDuet-1 plasmid used to clone *phnA1a* and *phnA2a*. Image retrieved from www.merck-chemicals.com/life-science-research, September 10th, 2010.

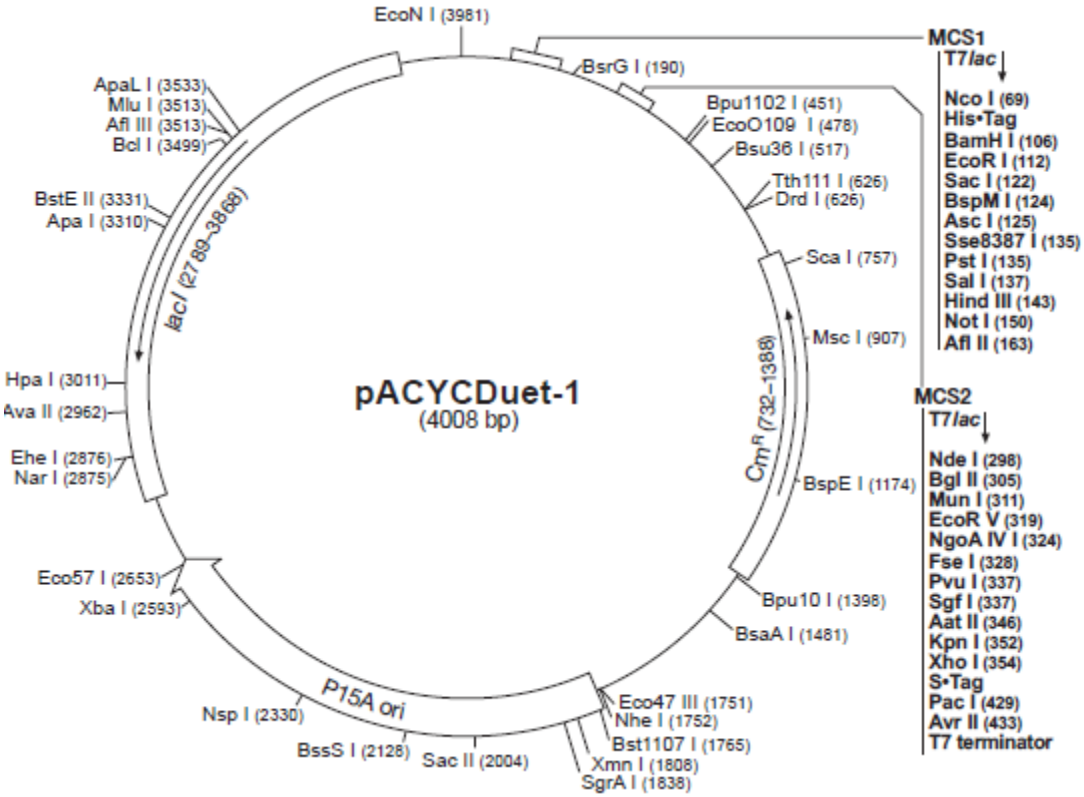

Figure 2.2 Vector map of the pACYCDuet-1 plasmid used to clone *phnA3* and *phnA4*. Image retrieved from www.merck-chemicals.com/life-science-research, September 10th, 2010.

RESULTS

3.1 BAC Library/Overgo Probing of High Density Filters

A BAC library of *Sphingomonas paucimobilis* EPA505 was constructed at the Clemson University Genomics Institute. Hybridization was carried out using oligonucleotide probes designed from partial sequences obtained in previous experiments (40). Following hybridization with the probe designed from a partial dioxygenase, numerous positive spots were identified (Fig. 3.1). A few positive clones were randomly picked from the library for further analysis.

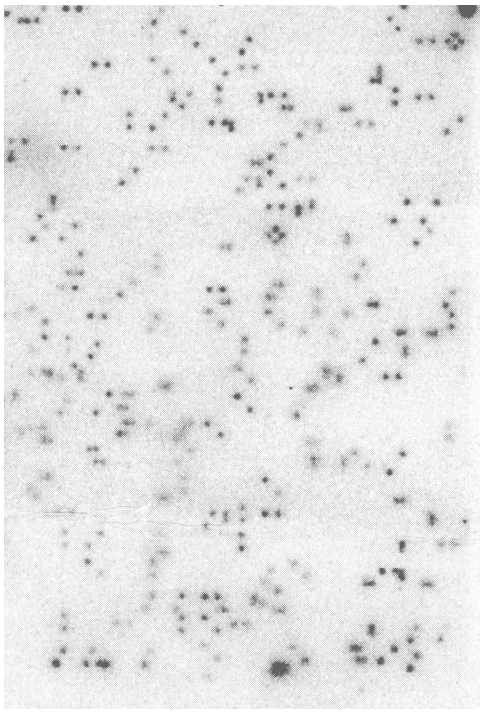

Figure 3.1 Overgo probing of high density BAC filters. Dark dots indicate positive hybridization to dioxygenase probe. Dot pattern indicates the location of the clone in the library.

3.2 Southern Analysis of BACs

DNA from the selected clones was extracted (Fig. 3.2) and subjected to restriction digestion with BamHI and HindIII (Fig. 3.3). Southern blot analysis revealed potential dioxygenase genes in some of the BAC clones. Because of the strong signal, BAC clone #04NO4 was chosen to make a shotgun library (Fig. 3.5). After this selection process, a shotgun library was constructed for high-throughput sequencing.

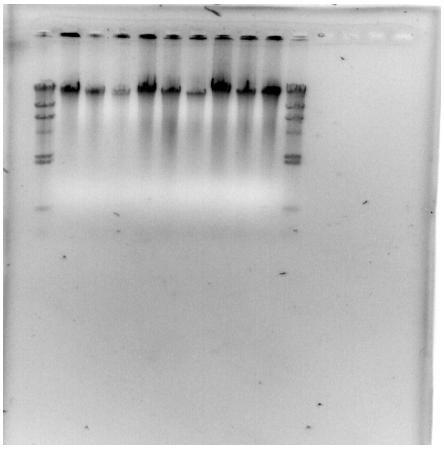

Figure 3.2 Agarose gel electrophoresis of DNA purified from selected BAC clones.

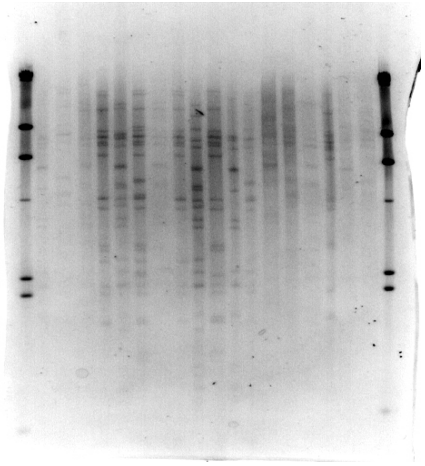

Figure 3.3 Agarose gel electrophoresis of digested BAC clones. After the marker in the first lane, every two lanes represent one BAC clone digested with BamH1 in the first and HindIII in the second lane.

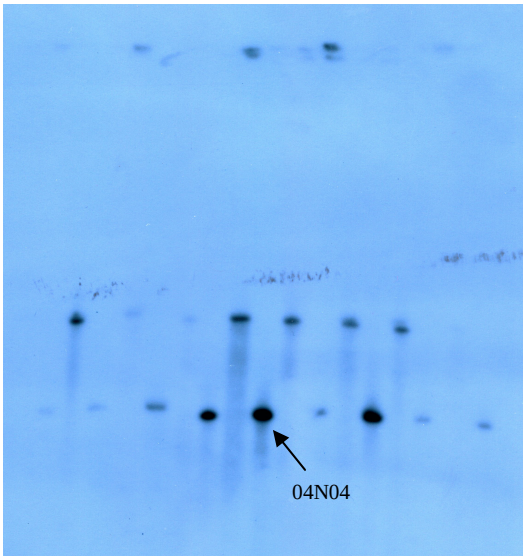

Figure 3.4 Southern analysis of digested BAC clones. Membrane was probed with overgos designed from partial dioxygenase gene sequences. Based on the strong signal, BAC #04N04 was chosen for shotgun cloning.

3.3 Sequencing Analysis

A shotgun library was constructed from one BAC clone which revealed dioxygenase genes following Southern analysis. After construction, the shotgun clones were subjected to high throughput sequencing using universal priming sites on the cloning vector. After all sequence data was collected, a total of 15 contigs were assembled. The results of BLAST similarity searches for contigs which revealed putative genes are listed in Table 3.1. Several different dioxygenases were identified. However, only three putative genes were selected for further analysis.

The first two genes were located on the same contig and showed 99% similarity to the *phnA1a* and *phnA2a* genes of *Sphingomonas* CHY-1 (Fig. 3.5). These two genes encode the alpha and beta subunits of an oxygenase. This contig also contained the aryl alcohol dehydrogenase *phnB*. A third gene was found on another contig and was 99% similar to the *bphA3* of *Sphingomonas* CHY-1. This gene encodes a ferredoxin and will be referred

to as *phnA3*. The *phnA3* gene was found on a contig containing other dioxygenase genes which were not selected for further analysis (Fig. 3.6 and Table 3.1).

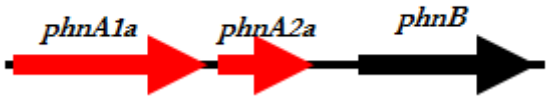

Figure 3.5 Schematic diagram of the contig containing *phnA1a* and *phnA2a*. The two oxygenase components are adjacent to one another and are followed by the aryl alcohol dehydrogenase gene, *phnB*.

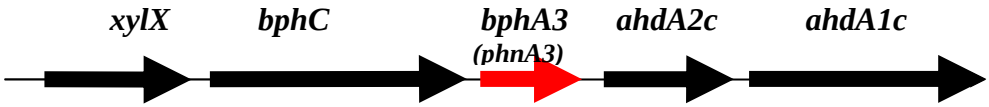

Figure 3.6 Schematic diagram of the contig containing *phnA3*. The gene encoding the ferredoxin component is preceded by two dioxygenase genes *xylX* and *bph* and is followed by genes encoding the small (*ahdA2c*) and large (*ahdA1c*) subunits of an oxygenase.

According to the literature (38), a fourth gene encoding a ferredoxin reductase subunit is necessary to complete the electron transport chain of the ring-hydroxylating dioxygenase enzyme. However, this gene was not identified in the sequencing results of the shotgun library. In order to find this gene, multiple rounds of PCR and sequencing were carried out using primers designed from conserved regions of bacterial ferredoxin reductase genes and using 04N04 BAC DNA as a template. After primer walking the complete sequence of a fourth subunit was positively identified as it was found to be 100% similar to the *ahdA4* gene of *Sphingomonas* sp. P2, which encodes a ferredoxin reductase. The ferredoxin reductase subunit of EPA505 found here will be referred to as *phnA4*. These four genes, i.e. *phnA1a*, *phnA2a*, *phnA3* and *phnA4* encode protein products which are components that make up a complete ring-cleaving dioxygenase enzyme shown to degrade both high and low molecular weight PAHs (38).

The ProtParam tool at the Expasy Proteomics server was used to determine the protein product size for each gene of interest. The gene encoding the alpha oxygenase component, *phnA1a*, is 1365bp long and was predicted to encode a protein consisting of 454 amino acids with a molecular weight of approximately 50 kD in size. PhnA1a contains more negatively charged residues than positively charged residues and is considered a stable protein with an instability index of 28.12. The gene encoding the beta subunit, *phnA2a*, is 525bp long. The protein product for this gene was predicted to be 174 amino acids long and approximately 21 kD in size. The amino acid composition for PhnA2a shows this protein as having more negatively charged residues. It also estimates an instability index of 47.35, classifying this protein as unstable. With regard to *phnA3*, a 327bp gene, the protein product was estimated to be 11.5 kD and 108 amino acids in length. The amino acid composition shows more negative than positive residues and an instability index of 41.16, classifying this protein as unstable. Lastly, the 1227bp gene *phnA4* encoding the ferredoxin reductase subunit, was estimated to be 408 amino acids in length and 44 kD in size. The protein product for this gene was estimated to have more negatively charged residues and an instability index of 31.05 making this protein stable.

Phylogenetic analysis revealed that the PhnA1a and PhnA2a subunits of EPA505 are most closely related to the alpha and beta terminal oxygenase components of *Sphingomonas* CHY-1 as was consistent with the BLAST results (Fig 3.18 and 3.19). Other closely related terminal oxygenase components include the PhnA1f and PhnA2f of *Sphingomonas* sp. LH128, the ArhA1 and ArhA2 subunits of Sphingomonas sp. A4, and the BphA1f and BphA2f subunits of *Sphingomonas yanoikuyae* B1 (54-56).

A multiple sequence alignment was done to compare the amino acid sequences of the alpha and beta subunits of EPA505 to those of related organisms. When the beta subunit PhnA2a was compared to the small subunit of the terminal oxygenase in six other organisms, the alignment revealed that some but not most amino acids were conserved (Fig. 3.21). When a multiple sequence alignment was done for PhnA1a, however, many residues were conserved among the sequences compared (Fig. 3.20). Conserved residues of significance include the six histidines and two cysteines which are thought to play a role in the [2Fe-S] cluster of the alpha subunit (41) and the Asp205 which is believed to connect the active site iron center of one alpha subunit to another (57, 58).

3.4 Cloning and protein expression

After the complete sequences of these four genes were identified, each gene was amplified separately to include appropriate restriction sites for cloning. Genes *phnA1a* and *phnA2a* encoding the oxygenase components were cloned into pETDueT-1 to give pD12. Genes *phnA3* and *phnA4* encoding the ferredoxin components were cloned into pACYCDuet-1 to yield the plasmid pACD34. In addition to these plasmids, expression host cells were also transformed with the original vectors containing no insert to yield BL21(DE3)(pETDuet-1) and BL21(DE3)(pETDuet-1)(pACYCDuet-1). These transformants were used as controls.

BL21(DE3) cells harboring either or both pD12 and pACD34 were grown and induced for expression. When BL21(DE3)(pD12) expressing only the two oxygenase components was induced and the cell lysate was analyzed by SDS-PAGE, a 53 kD band

and a 21 kD band was seen in the induced culture as compared to the uninduced cells. These two bands represent the recombinant *phnA1a* and *phnA2a* gene products, respectively (Fig3.7). Following induction of BL21(DE3)(pD12)(pACD34) expected to express all four subunits, SDS-PAGE analysis revealed two prominent bands at the expected sizes of the *phnA1a* and *phnA2a* products (Fig3.8). However, no representative bands were seen for the ferredoxin or ferredoxin reductase components.

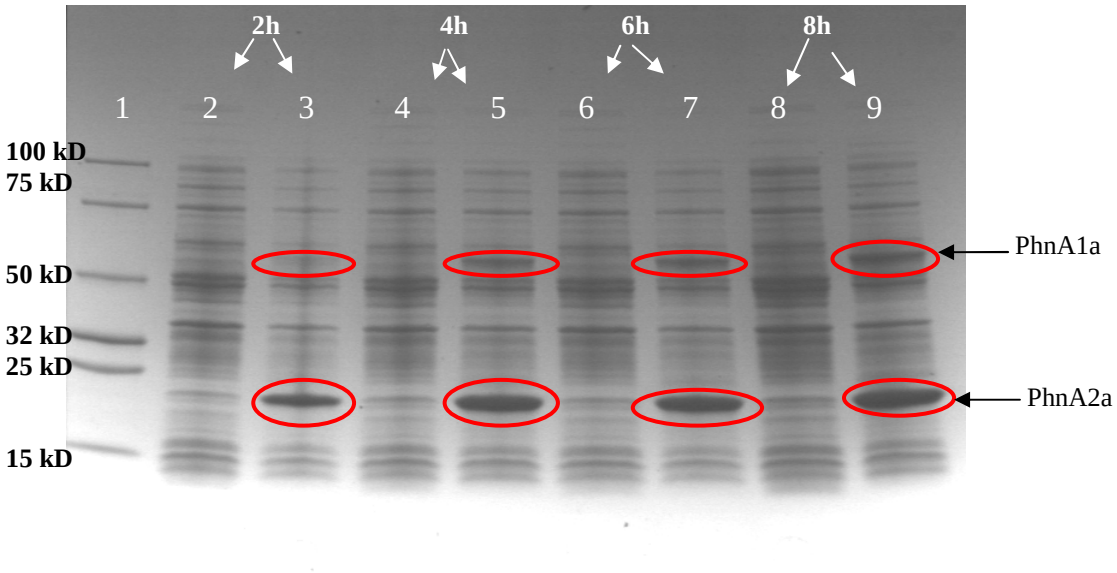

Figure 3.7 SDS-PAGE analysis of induced BL21(DE3) cells harboring pD12. A protein ladder is loaded in lane 1. Odd numbered lanes are induced samples at the various time points following induction with IPTG. Even numbered lanes are the corresponding uninduced samples.

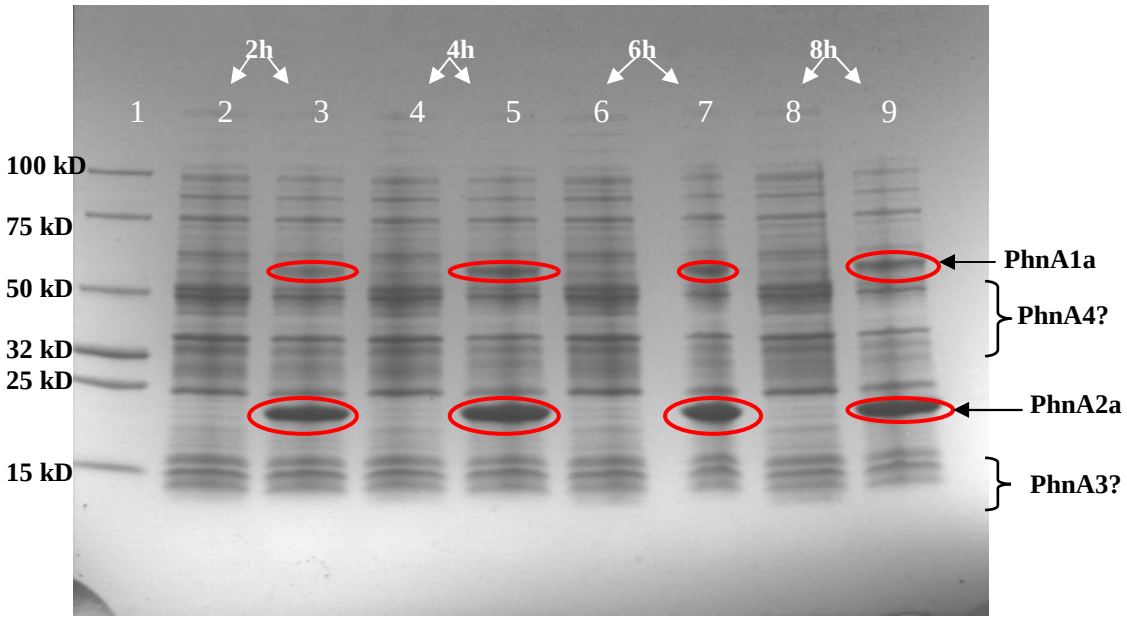

Figure 3.8 SDS-PAGE analysis of induced BL21(DE3) cells harboring both pD12 and pACD34. Protein ladder is loaded in lane 1. Samples in odd numbered lanes are induced and the corresponding uninduced samples are loaded in the even numbered lanes. Two prominent bands can be seen for PhnA1a and PhnA2a. No appropriately sized bands are present for PhnA3 and PhnA4.

Since no bands indicated the expression of the two ferredoxin subunits, pACD3 and pACD34 were introduced into the expression host to check expression levels in the absence of pD12. When BL21(DE3)(pACD3) cells carrying the plasmid with the *phnA3* gene only was induced for expression, a band of about 15 kD representing the cloned *phnA3* gene product was detected by SDS-PAGE. When BL21(DE3)(pACD34) carrying both *phnA3* and *phnA4* was induced, a 15 kD band indicative of the *phnA3* product was again seen. However, it was present in a lower concentration than when this gene was expressed alone. Additionally, there was a band below the 50 kD mark. This was presumed to be the 45 kD product of *phnA4* (Fig. 3.9).

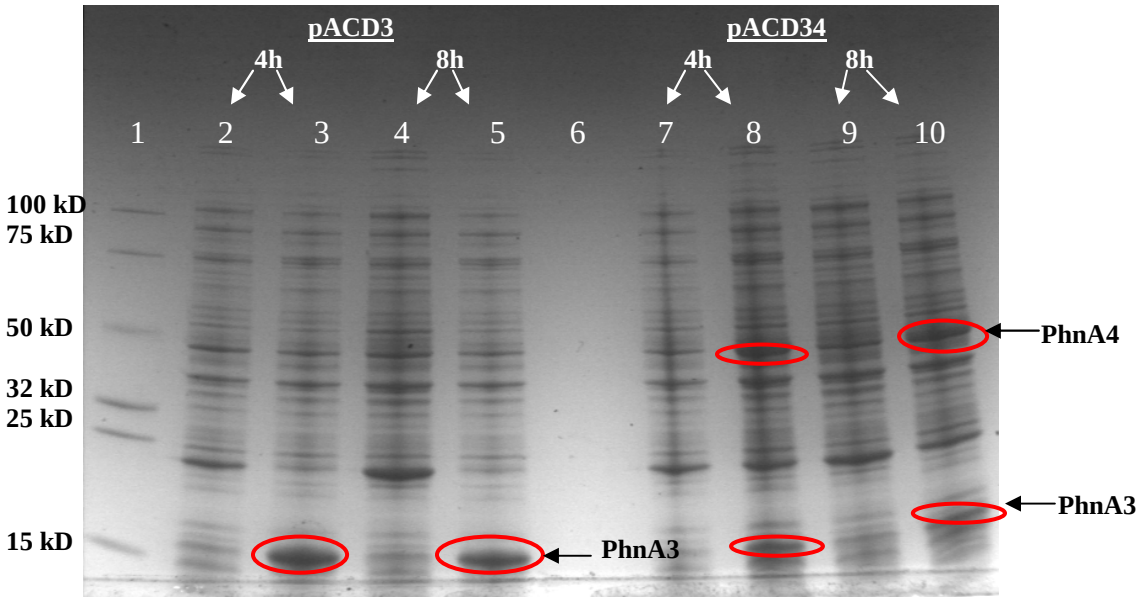

Figure 3.9 SDS-PAGE analysis of BL21(DE3) cells harboring only pACD3 (samples on the left) to express *phnA3* only, and pACD34 (samples on the right) expressing *phnA3* and *phnA4*. A protein ladder is loaded in lane 1. Uninduced samples are in lanes 2,4, 7 and 9. Induced samples are in lanes 3,5,8 and 10.

3.5 Assay for Recombinant Protein Activity

To test the enzyme activity of the recombinant proteins, all four dioxygenase components were expressed by inducing BL21(DE3)(pD12)(pACD34) with IPTG. The induced cells were then incubated with either naphthalene, phenanthrene, or fluoranthene. The results of the recombinant protein activity assay are summarized in Table 3.2.

When grown in the presence of naphthalene, a product was detected through GC-MS with a retention time of 15.73 minutes (Fig. 3.10). The EI mass spectrum (molecular ion at m/z 306) of this product was similar to the mass spectrum found previously for a trimethylsilylated naphthalene dihydrodiol production (45) (Fig. 3.11). In addition, no dihydrodiol product was found in the control.

When incubated with phenanthrene, GC-MS also detected a product indicating biotransformation of phenanthrene by the dioxygenase with a retention time of 21.67 minutes (Fig. 3.12). This product was identified as a phenanthrene dihydrodiol since it had the same fragmentation pattern (molecular ion at m/z 356) as the trimethylsilylated phenanthrene dihydrodiol previously described (45) (Fig. 3.13).

When cells expressing all four components of the dioxygenase were incubated with fluoranthene, no breakdown products were detected. However, unlike with naphthalene and phenanthrene, after several hours of incubation, fluoranthene was still detected in the supernatant of all cultures including the controls. This might indicate a problem with uptake of fluoranthene.

A second assay for fluoranthene was carried out using the cell lysate. Cells expressing all four proteins were induced overnight, harvested, resuspended in Tris buffer (pH 7.5) and lysed. Fluoranthene was then added to the cell lysate. GC-MS did not detect any fluoranthene dihydrodiol products in the lysate samples.

The activity of BL21(DE3)(pD12) expressing only the PhnA1a and PhnA2a oxygenase components was also tested. When these cells were incubated with naphthalene, phenanthrene, and fluoranthene, no breakdown products were detected by GC-MS. No fragments were detected to indicate the presence of dihydrodiols for any of the substrates tested.

Table 3.2 Summarized results of the recombinant protein activity assay for BL21(DE3)(pD12)(pACD34) induced cells expressing all four subunits of the multi-component dioxygnease.

Expressed Proteins	Compound	Product Identified	RT (min)	Ionization fragments
Control	Naphthalene	------	15.73	-----
A1aA2aA3A4	Naphthalene	Naphthalene dihydrodiol	15.73	73, 147, 191, 203, 275, 306
Control	Phenanthrene	-------	21.67	-----
A1aA2aA3A4	Phenanthrene	Phenanthrene dihydrodiol	21.67	73, 147, 165,178, 251, 266, 309, 325, 341, 356
Control	Fluoranthene	--------	----	-----
A1aA2aA3A4	Fluoranthene	--------	----	-----

A

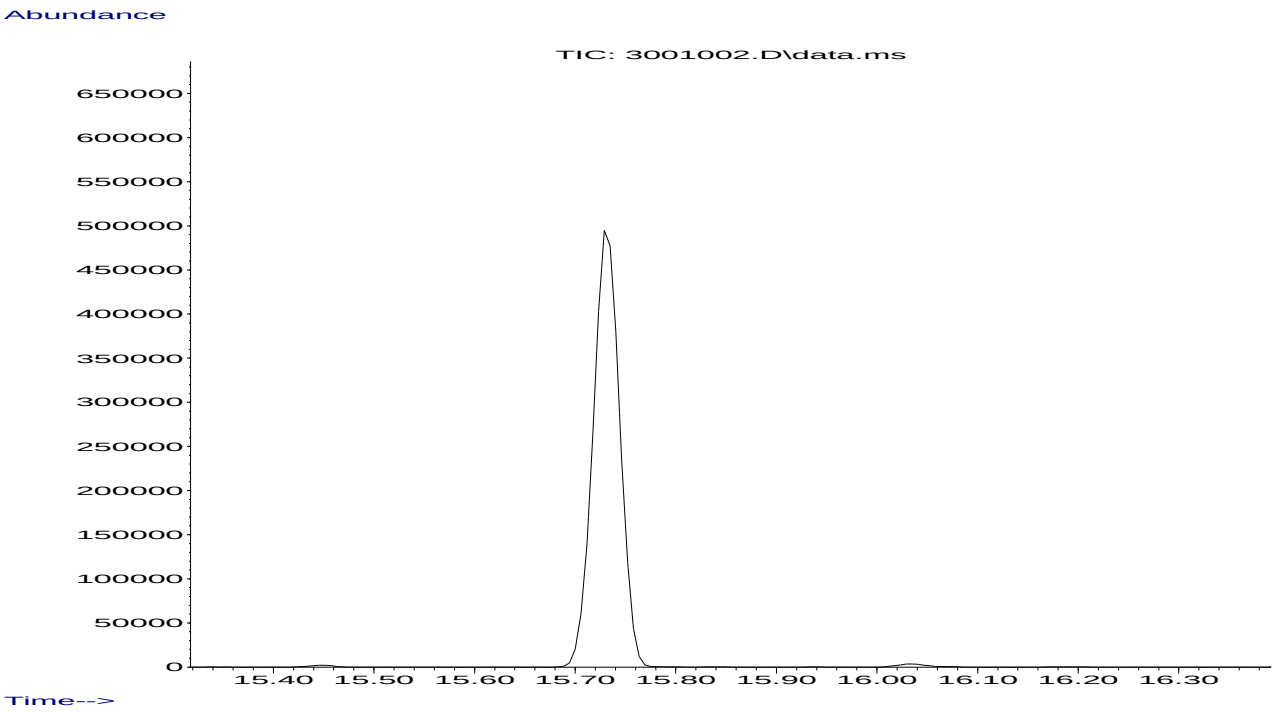

B

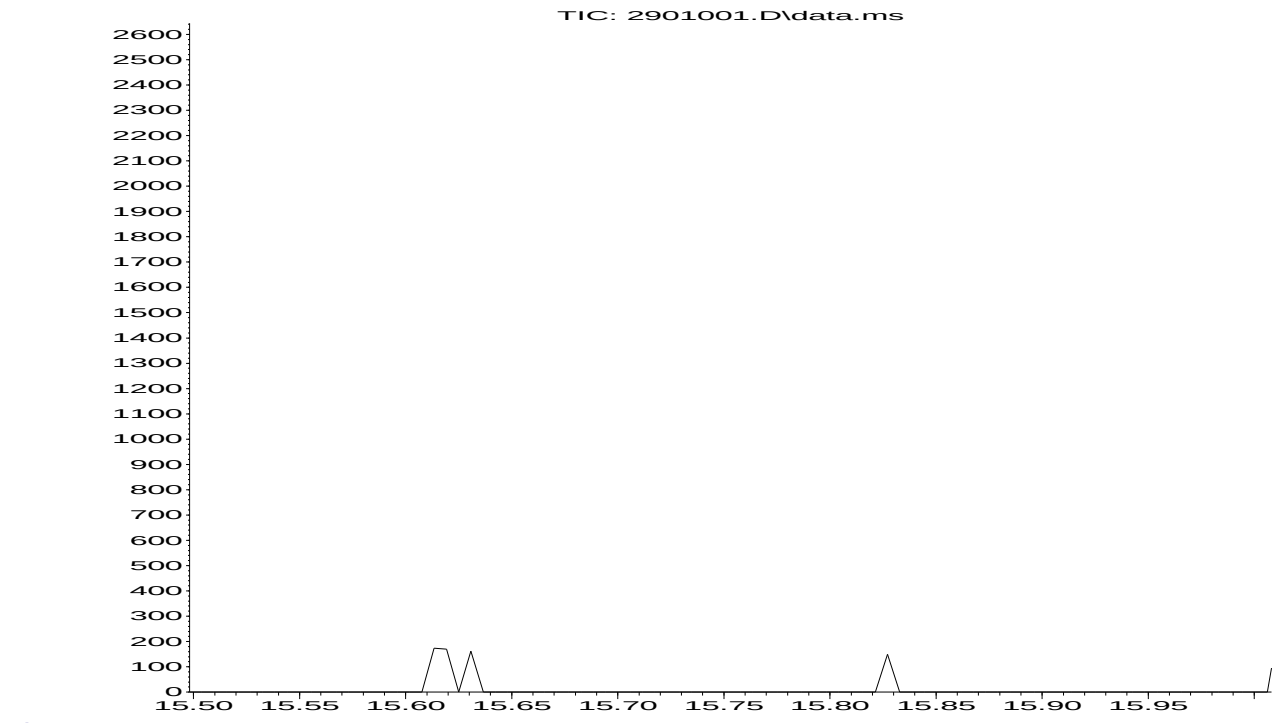

Figure 3.10 Extracted ion chromatograms of BL21(DE3)(pD12)(pACD34) and control cultures incubated with naphthalene. (A) A breakdown product was identified with a retention time of 15.73 minutes in cells expressing genes for all dioxygenase components. (B) No compound was identified in the control at the same retention time. Mass spec data confirmed the compound as a naphthalene dihydrodiol (see Fig 3.11).

A

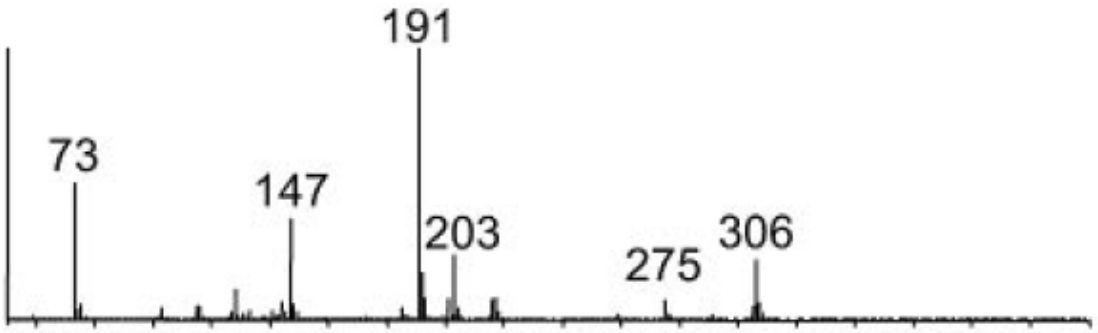

Kim et al., (2005)

B

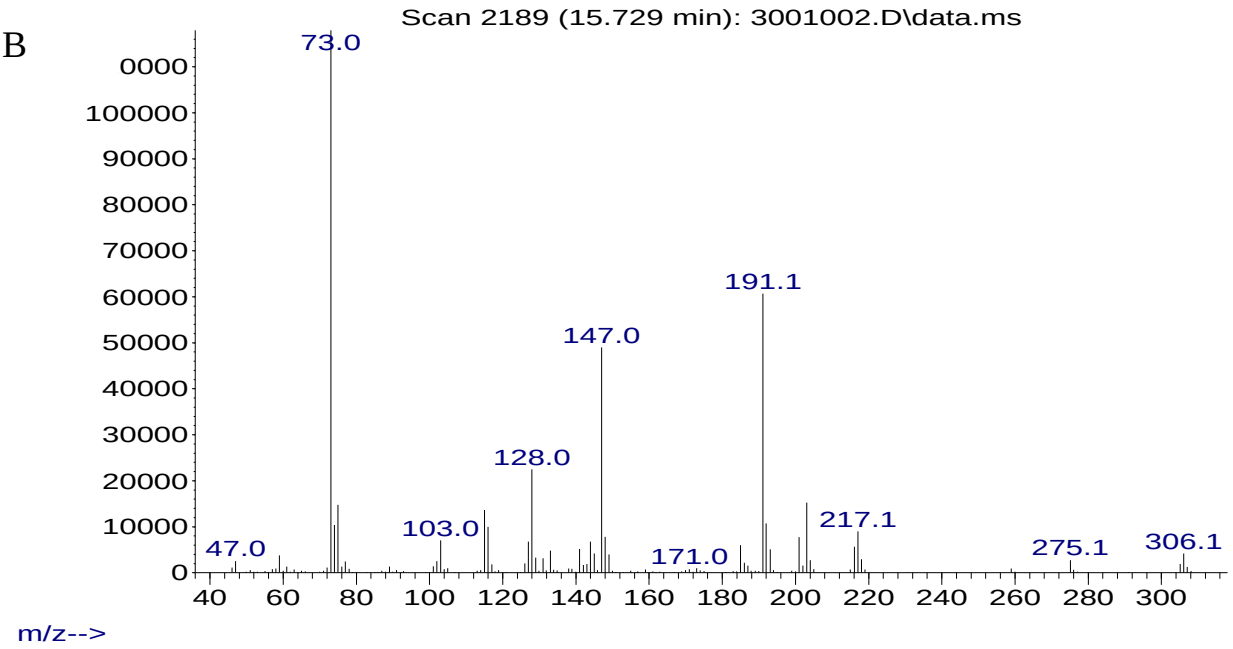

Figure 3.11 (A) EI mass spectrum of naphthalene dihydrodiol as described by Kim et al., (2005). (B) EI mass spectrum of compound identified at 15.73 minutes in BL21(DE3)(pD12)(pACD34) culture incubated with naphthalene. Similar fragmentation patterns positively identified this compound as a naphthalene dihydrodiol.

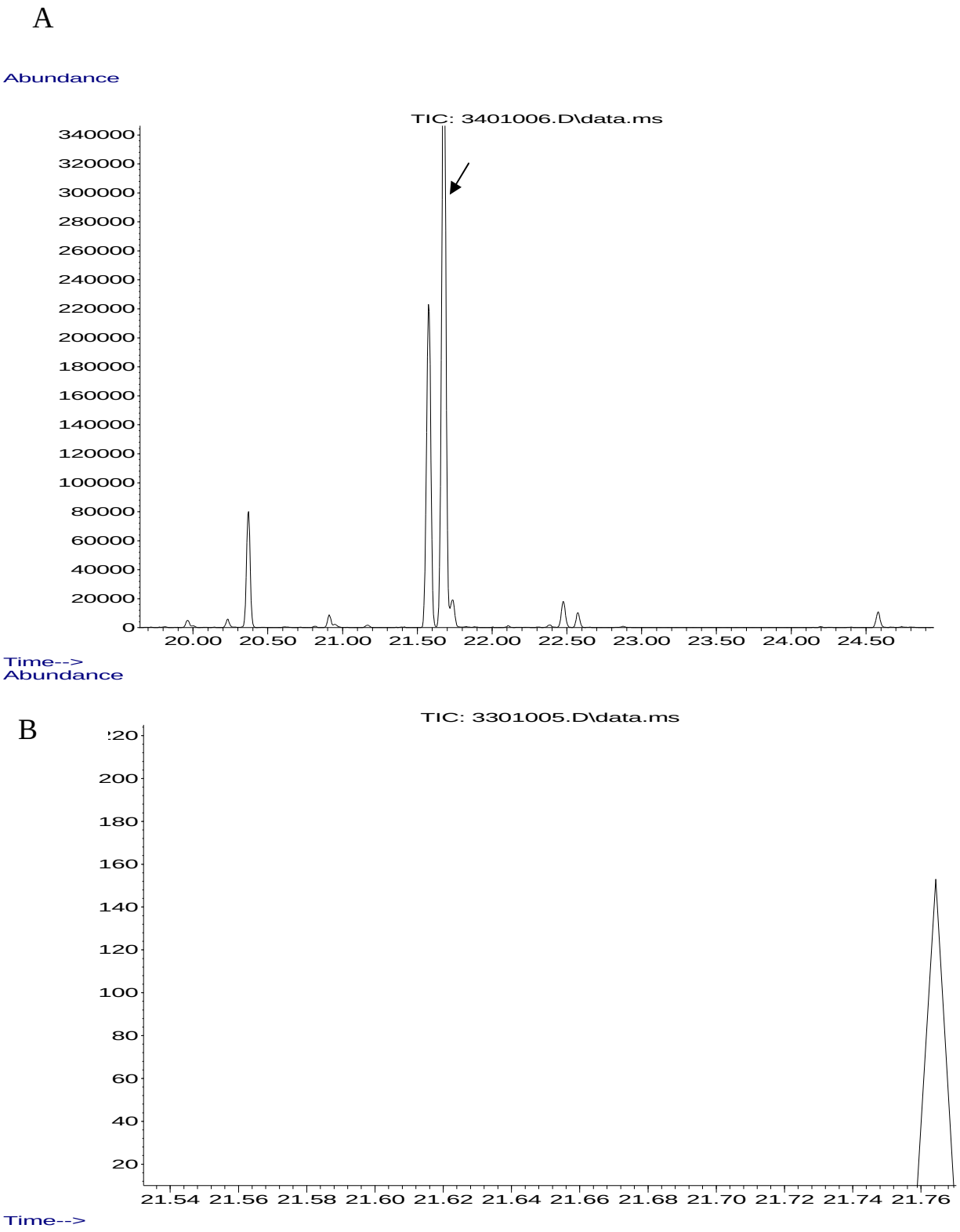

Figure 3.12 Extracted ion chromatograms of cultures incubated with phenanthrene. (A) A compound identified at 21.67 minutes in cells expressing all four genes. (B) No compound was identified in the control at the same retention time.

A

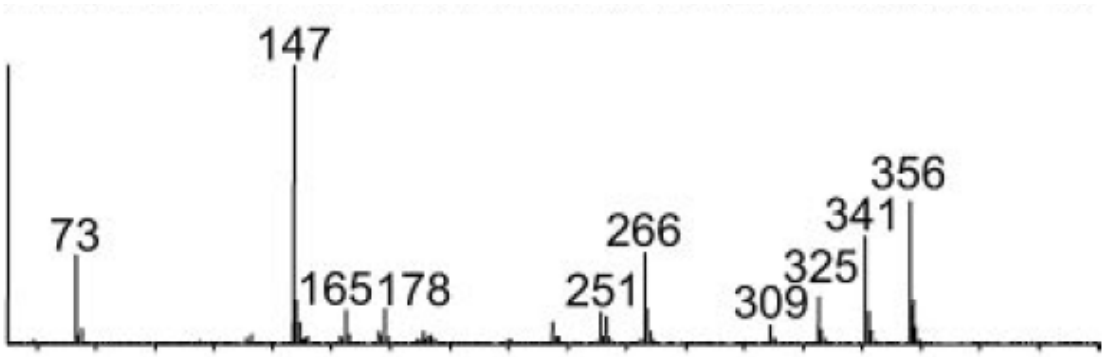

Kim et al., 2005.

B

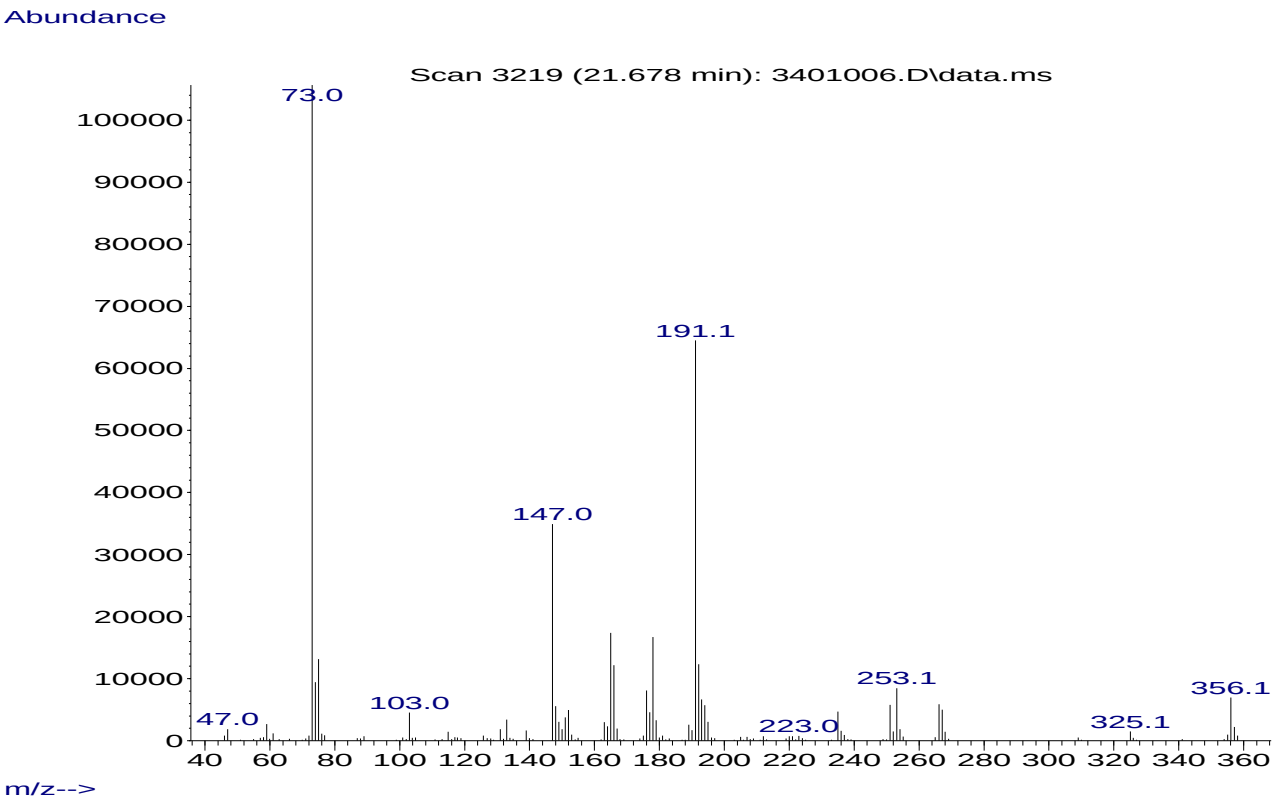

Figure 3.13 (A) EI mass spectrum of phenanthrene dihydrodiol (Kim et al., 2005). (B) EI mass spectrum of the compound identified in BL21(DE3)(pD12)(pACD34) phenanthrene culture with a retention time of 21.67 minutes. The similar fragmentation pattern confirms this compound as a phenanthrene dihydrodiol.

atgagcggcgacaccacactcgtagacactgtcaatgctagccagtcccgtcaggtgttc
M S G D T T L V D T V N A S Q S R Q V F
tgggacagagacgtttatgatcttgaaatagagcggatttttcccgggcatggttgatg
W D R D V Y D L E I E R I F S R A W L M
ctcggccacaaatcgcttctcccgaagccgggcgacttcatcacgacttatatggccgag
L G H K S L L P K P G D F I T T Y M A E
gacaagatcatcctttcgcaccagagcgacgggaccttccgcgcctttatcaattcgtgc
D K I I L S H Q S D G T F R A F I N S C
acgcaccgcggcaaccagatttgccacgccgacagcggtaacgccaaggcgttcgtctgc
T H R G N Q I C H A D S G N A K A F V C
aattatcacggctgggtgtacgggcaggatggatcgttggtcgatgtcccactcgagtcg
N Y H G W V Y G Q D G S L V D V P L E S
cgctgttaccacaacaaactcgataagcaagagctggcggcgaagtctgttcgggtcgaa
R C Y H N K L D K Q E L A A K S V R V E
acctacaagggtttcattttcggttgccatgatcccgaagcgccaagccttgaagactac
T Y K G F I F G C H D P E A P S L E D Y
ctgggcgaattccgtttttatctcgacaccatctgggaaggaggggcgctgggctggaa
L G E F R F Y L D T I W E G G G A G L E
ctgctcggtccgccgatgaagagcctgcttcactgcaactggaaagtgccggtcgaaaat
L L G P P M K S L L H C N W K V P V E N
tttgtcggcgacggatatcatgtcggatggacccatgcggcggcgcttggtcagatcggt
F V G D G Y H V G W T H A A A L G Q I G
ggtctgtttgcgggactggccggcaaccgcgcggacattcccttcgacgatcttggattg
G L F A G L A G N R A D I P F D D L G L
cagttcacgacccggcatggtcatggctttgggttggtcgacaacgcggcggctgcgatc
Q F T T R H G H G F G L V D N A A A A I
caccgaaagggcgacggctggaacaaatatcttgaggacacccgcggcgaggtgcgccgc
H R K G D G W N K Y L E D T R G E V R R
aagtttggcgcggatcgcgaacggctttatgtcgggcactggaacggcgcgatcttcccc
K F G A D R E R L Y V G H W N G A I F P
aattgctcgttcctgtatggcaccaacaccttcaaaatctggcatccacgcgggccgcac
N C S F L Y G T N T F K I W H P R G P H
gagattgaagtatggacctataccatggtgccgagcgatgccgatcccgctaccaagagt
E I E V W T Y T M V P S D A D P A T K S
gcgatacagcgcgaagcgacgagaacattcggaaccgccgggacgctggaaagcgacgac
A I Q R E A T R T F G T A G T L E S D D
ggcgaaaacatgtcttcggcaacctacgtgaaccgtggcgtgatcacgcgtgacggcatg
G E N M S S A T Y V N R G V I T R D G M
atgaattcgaccatgggcgtcggctacgaaggaccgcatccggtttatcccggaatcgtc
M N S T M G V G Y E G P H P V Y P G I V
ggcatcagcttcattggcgagacatcctaccggggcttctaccggttctggaaggaaatg
G I S F I G E T S Y R G F Y R F W K E M
atcgatgcccccgattgggcgagcgtgaaggcaaacgacgacaattgggattcggtcttc
I D A P D W A S V K A N D D N W D S V F
acgaatcgcaatttctggaacgaaaagctcaacgcggccgaatga
T N R N F W N E K L N A A E -

Fig. 3.14 Complete *phnA1a* nucleotide and amino acid sequence

```
atgtcgaccgaacaagttccggtgacgccggatgtgcactacgccgtcgaagcgcactat
 M  S  T  E  Q  V  P  V  T  P  D  V  H  Y  A  V  E  A  H  Y
cgtgccgaggtcagactgttgcagaccgggcagtaccgggaatggctgcacggaatggtc
 R  A  E  V  R  L  L  Q  T  G  Q  Y  R  E  W  L  H  G  M  V
gccgaagacatccattactggatgccgatttacgaacagcgcttcgtgagagaccggcgc
 A  E  D  I  H  Y  W  M  P  I  Y  E  Q  R  F  V  R  D  R  R
ccggacccaacgccagacgatgcggcaatttacaacgacgacttcgaagagctcaagcag
 P  D  P  T  P  D  D  A  A  I  Y  N  D  D  F  E  E  L  K  Q
cgtgtcgaacggctttattcaggtcaggtctggatggaggatccgccatccaaaatccgg
 R  V  E  R  L  Y  S  G  Q  V  W  M  E  D  P  P  S  K  I  R
tacttcgtgtcgaatgtcgaagcctttgaagccgaaaacggcgaattggacgtcctgtcg
 Y  F  V  S  N  V  E  A  F  E  A  E  N  G  E  L  D  V  L  S
aacatccttgtctaccgcaaccgccgccagactgaagtcacggtgcatacattggggcgt
 N  I  L  V  Y  R  N  R  R  Q  T  E  V  T  V  H  T  L  G  R
gaagacaagttgcgccaggacggcaatggtttcaaggtcttccggcgaaaacttatcctc
 E  D  K  L  R  Q  D  G  N  G  F  K  V  F  R  R  K  L  I  L
gatgcgagagtcacgcaagacaagaatctgtatttcttttgttag
 D  A  R  V  T  Q  D  K  N  L  Y  F  F  C  -
```

Fig. 3.15 Complete *phnA2a* nucleotide and amino acid sequence

```
atgtcgaacaaactgcgcctttgccaagtagcggacgttaaggatggtgaacctgtcgcg
 M  S  N  K  L  R  L  C  Q  V  A  D  V  K  D  G  E  P  V  A
gtttaccaggagcaaatgcctgcgcttgccgtctacaacgtcgatggcgatgtattcgtc
 V  Y  Q  E  Q  M  P  A  L  A  V  Y  N  V  D  G  D  V  F  V
accgacaatatgtgcacccatggcaatgccatgctgaccgatggctaccaggacggcgga
 T  D  N  M  C  T  H  G  N  A  M  L  T  D  G  Y  Q  D  G  G
atcatcgaatgcccgttccatggtggttccttcgacatcgccaccggagcagccaaagcc
 I  I  E  C  P  F  H  G  G  S  F  D  I  A  T  G  A  A  K  A
tttccctgccaggttccgatcaagacctactcagtcacgatcgacgacggctgggtgtgc
 F  P  C  Q  V  P  I  K  T  Y  S  V  T  I  D  D  G  W  V  C
atcgatcagccggaagggagcgcctga
 I  D  Q  P  E  G  S  A  -
```

Fig. 3.16 Complete *phnA3* nucleotide and amino acid sequence

```
gtgcgctcgattgctatagttggtgcaaacctggccggtgggcgcgcagtcgaagccctg
 V  R  S  I  A  I  V  G  A  N  L  A  G  G  R  A  V  E  A  L
cggcaggcagggttcgacgggcggatcaccttgatcggcgaagaaccgtggcgtccttat
 R  Q  A  G  F  D  G  R  I  T  L  I  G  E  E  P  W  R  P  Y
gaacggccgccgctctccaaggaagtgctgtgggaaccggcaaatgttccggacaatttc
 E  R  P  P  L  S  K  E  V  L  W  E  P  A  N  V  P  D  N  F
ttcctgcaggacgaggcctggtacgacgataaccgtatcgacatgcgcctgggcacccga
 F  L  Q  D  E  A  W  Y  D  D  N  R  I  D  M  R  L  G  T  R
gccgaagcaatcgaccttgcgagcggcggggtccgcctgtcaggggcgagctggttcag
 A  E  A  I  D  L  A  S  G  G  V  R  L  S  G  G  E  L  V  Q
gcggaccggatcctgctcgccacgggcggtcacgcccgcaagctcaaccttgccggggcc
 A  D  R  I  L  L  A  T  G  G  H  A  R  K  L  N  L  A  G  A
gattgcgagaacgtccattatctgcgcacacgagacgatgcgacccgcatggcgctcgac
 D  C  E  N  V  H  Y  L  R  T  R  D  D  A  T  R  M  A  L  D
ctgcgcgaaggtgccagcatcgtgatcgtcggcatgggcgtaatcggcgccgaagtcgcc
 L  R  E  G  A  S  I  V  I  V  G  M  G  V  I  G  A  E  V  A
gccagtgcggtaaaactcggctgcaaggtcaccgtcgtcgagccgatgccagtgccgatg
 A  S  A  V  K  L  G  C  K  V  T  V  V  E  P  M  P  V  P  M
gaaagagcgctcggccggcgctttgggcaatggctgggcgaggagcatcgcaggcgggga
 E  R  A  L  G  R  R  F  G  Q  W  L  G  E  E  H  R  R  R  G
gtagcgacccatttcaactgcggcgtgaccggcttcaggtttgccggcaaccgtgtcagc
 V  A  T  H  F  N  C  G  V  T  G  F  R  F  A  G  N  R  V  S
gcggtcgtggcagacgatggcaccgtgattccgtgcgatgccgtgatcgtgggggtgggg
 A  V  V  A  D  D  G  T  V  I  P  C  D  A  V  I  V  G  V  G
atcgtgccggccacctcgctggcccgcgatgccgggatcgaggtcaacaacgggatcatc
 I  V  P  A  T  S  L  A  R  D  A  G  I  E  V  N  N  G  I  I
gtcgaccgtcgatgccagaccagcaacccggcggtattcgcggcgggcgacgtggccgag
 V  D  R  R  C  Q  T  S  N  P  A  V  F  A  A  G  D  V  A  E
caggacgggtttttcggcggacggttcaggcaggaaacctaccagaacgctgccgaccag
 Q  D  G  F  F  G  G  R  F  R  Q  E  T  Y  Q  N  A  A  D  Q
gcgcaggcgggcgccctggcgatgctggggcaggaggtctcctactgcaagccgatgtgg
 A  Q  A  G  A  L  A  M  L  G  Q  E  V  S  Y  C  K  P  M  W
tactggagcgatcagttcgatctcaacatccagttctgcgggcaaattcccgtagaagcc
 Y  W  S  D  Q  F  D  L  N  I  Q  F  C  G  Q  I  P  V  E  A
gatatcgcaattcgcggcgagatggacagcaacaccttcgtcgccttcttcctggccggt
 D  I  A  I  R  G  E  M  D  S  N  T  F  V  A  F  F  L  A  G
gaaacgatcgaaggcgtactgacggtcaaccgcgcgcccgacatgggggtgggcaagcgg
 E  T  I  E  G  V  L  T  V  N  R  A  P  D  M  G  V  G  K  R
ctcgtcgaaaggcgagcccgcgccagcgccgcaagcctggcagacgccaatgtttccttg
 L  V  E  R  R  A  R  A  S  A  A  S  L  A  D  A  N  V  S  L
cgggacttgctcaagcaggcgggctga
 R  D  L  L  K  Q  A  G  -
```

Fig 3.17 Complete *phnA4* nucleotide and corresponding amino acid sequence. Unlike the other subunits, PhnA4 starts with a valine.

Table 3.1 Significant BLAST search results of contigs assembled after sequencing shotgun clones.

Contig #	Database match	Organism	% Identity	Accession no.
#1				
1-756bp	Tni-B like transposition protein	*Sphingomonas* sp. KA1	65%	YP 718159.1
805-1518bp	hypothetical protein pCAR_219	*Sphingomonas* sp. KA1	35%	YP 718160.1
#3				
1465-2193bp	plasmid stabilization protein	*Sphingomonas* sp. KA1	82%	YP 718143.1
#4				
1-405bp	hydroxythreonine-4-phosphate dehydrogenase	Sphingobium yanoikuyae	91%	ABM79787.1
416-970bp	toluene/benzoate dioxygenase small subunit	Sphingomonas sp. DN1	89%	ACV31387.1
#5				
310-1014bp	putative transposase	Sphingomonas sp. SKA58	55%	ZP 01301940.1
#6				
4-1035bp	transposase Tn3 family protein	Ochrobactrum anthropi	73%	YP 001373193.1
#7				
320-1288bp	2-hydroxy-benzylpyruvate aldolase	*Sphingomonas* sp. P2	90%	BAC65452.1
#8				
3-407bp	hypothetical protein pCAR_211	*Sphingomonas* sp. KA1	92%	YP 718152.1
469-1152bp	putative methylase/helicase	*Sphingomonas* sp. KA1	92%	YP 718151.1
#9				
2-862bp	large subunit of oxygenase	*Sphingomonas* sp. P2	92%	BAC65433.1
1062-1538bp	salicylate 1-hydroxylase beta subunit	Sphingobium yanoikuyae	94%	ABM79789.1
1591-2190bp	chain A, Sphingomonad Glutathione S-transferase	Sphingomonads	77%	1F2E_A
#10				
71-1324bp	putative partitioning protein ParA	*Sphingomonas* sp. KA1	99%	YP 718154.1
#11				
1-1035bp	3-isopropylmalate dehydrogenase	*Novosphingobium aromaticivorans*	82%	NP 049056.1
#12				
1079-2444bp	alpha subunit, ring-hydroxylating dioxygenase, *phnA1a*	*Sphingomonas* sp. CHY-1	100%	AJ63551.1
2488-3013bp	beta subunit, ring-hydroxylating dioxgenase, *phnA2a*	*Sphingomonas* sp. CHY-1	100%	AJ63551.1
3059-3083bp	partial aryl alchohol dehydrogenase, *phnB*	*Sphingomonas* sp. CHY-1	100%	AJ63551.1
#13				
2-550bp	large subunit oxygenase	*Sphingomonas* sp. P2	96%	BAC65453.1
550-1044bp	small subunit oxygenase	*Sphingomonas* sp. P2	93%	BAC65454.1
1114-2115bp	amidohydrolase 2	*Burkholderia* sp. H160	45%	ZP 03266800.1
2614-3618bp	demethylmenaquinone methyltransferase protein	*Ralstonia solanacearum* MolK2	40%	CAQ37090.1
#14				
219-865bp	putative large subunit toluene/benzoate dioxygenase, *xylX*	*Sphingomonaspaucimobilis*	99%	FM882255.1
1154-2054bp	putative biphenyl-2,3-diol 1,2-dioxygenase, *bphC*	*Spingomonas paucimobilis*	99%	FM882255.1
2104-2430bp	putative ferredoxin component of dioxygenase, *bphA3*	*Spingomonas paucimobilis*	99%	FM882255.1
2431-2919bp	putative small subunit of oxygenase, *ahdA2c*	*Spingomonas paucimobilis*	99%	FM882255.1
2942-3742bp	partial putative large subunit of oxygenase, *ahdA1c*	*Spingomonas paucimobilis*	99%	FM882255.1
#15				
2667-4349bp	putative cation efflux system protein	*Pseudomonas aeruginosa*	69%	YP790640.1

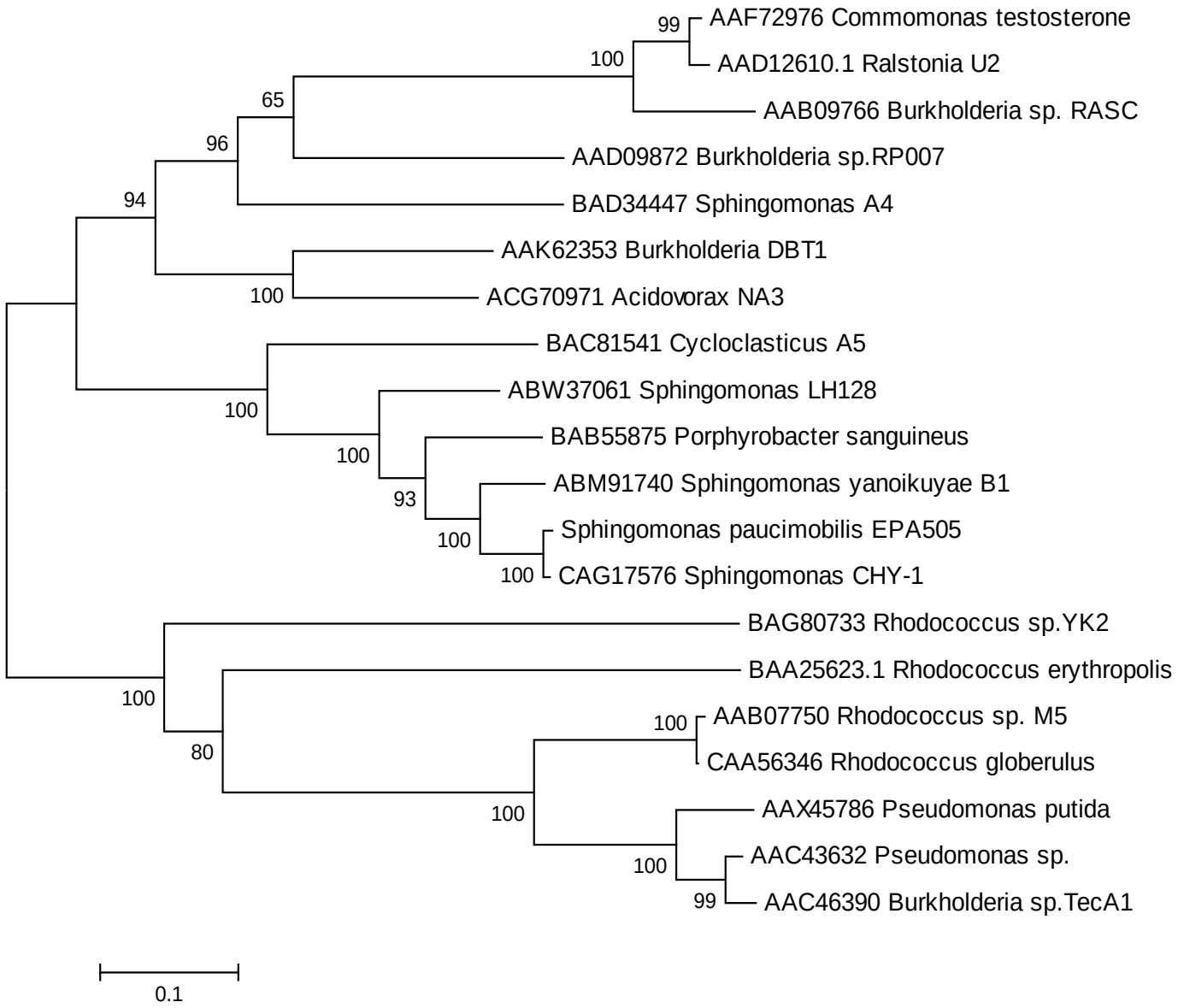

Fig 3.18 Phylogenetic tree showing the relationship of the alpha subunit PhnA1a and related alpha subunits of various organisms. Tree was constructed with MEGA version 4.0.

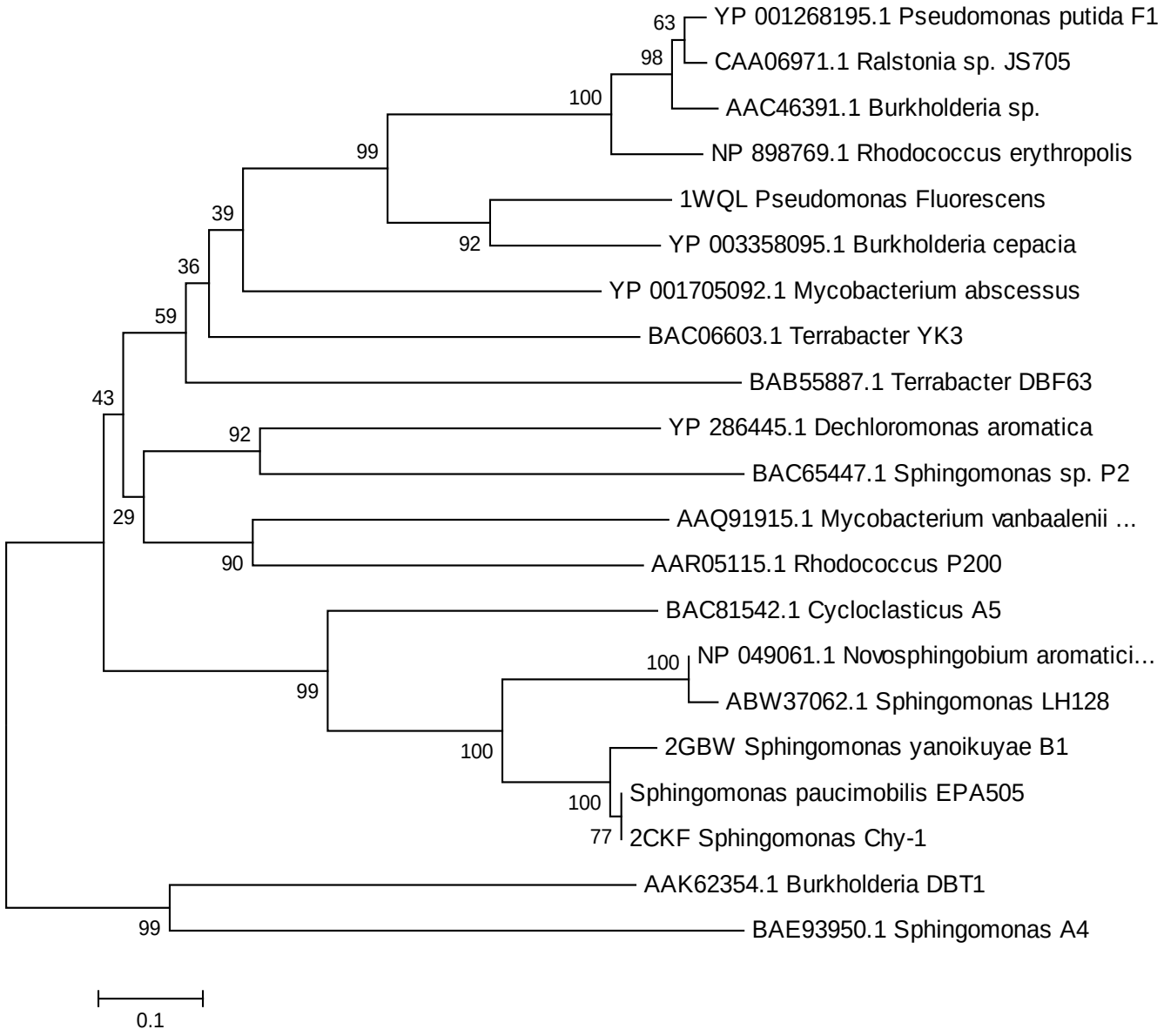

Fig. 3.19 Phylogenetic tree showing the relationship of the beta subunit PhnA2a to other known terminal oxygenase small subunits. Tree was constructed using MEGA 4.0.

```
EPA505  MSGDTTLVDTVNASQSRQVFW-DRDVYDLEIERIFSRAWLMLGHKSLLPKPGDFITTYMA 59
CHY-1   MSGDTTLVDTVNASQSRQVFW-DRDVYDLEIERIFSRAWLMLGHKSLLPKPGDFITTYMA 59
S.y B1  MSSDATLVDTVNASQSRQVFW-DEDVYALEIERIFSRAWLMLGHESLVPKPGDFITTYMA 59
S.LH128 MNGSSALVDNAGASQSRRVFW-DQDVYQLELERIFSRCWLMLGHDSLVPKPGDFITTYMA 59
C.A5    MVDINKLVDTKASTQSKEVFW-DQEVYDREIKNIFGRSWLFLTHECMLEKKGDFITTKMA 59
S.A4    ---MDDLIDTKRGLQSASMFI-DPHLYEVEMEKIFGRCWLFLTHESAIPNYGDFVTAKMG 56
P.NDO   MNYNNKILVSESGLSQKHLIHGDEELFQHELKTIFARNWLFLTHDSLIPAPGDYVTAKMG 60
              :: .  . ..  ::  * .::  *:: **.* **:* *.. :   **::*: *.

EPA505 EDKIILSHQSDGTFRAFINSCTHRGNQICHADSGNAKAFVCNYHGWVYGQDGSLVDVPLE 119
CHY-1  EDKIILSHQSDGTFRAFINSCTHRGNQICHADSGNAKAFVCNYHGWVYGQDGSLVDVPLE 119
S.y B1 EDKVILSHQSDGTFRAFINSCSHRGNQICHADSGNAKAFVCNYHGWVFGQDGSLVDVPLE 119
S.LH128EDRVILSRQPDGSLKAFINSCTHRGNQICHADSGSAKAFVCNYHGWVFGQDGSLVDVPME 119
C.A5   EDSVIVTRHTDGSLKAFVNSCTHRGNSICSADSGNTKSFVCNYHGWVFSTDGKLVDVPLR 119
S.A4   EDEVLVVRQEDGTVKAFLNVCRHRGARVCPVEAGNRRAFVCNYHGWSYAADGSLAAIPFE 116
P.NDO  IDEVIVSRQNDGSIRAFLNVCRHRGKTLVSVEAGNAKGFVCSYHGWGFGSNGELQSVPFE 120
        * ::: :: **:.:**:* * ***  :  .::*. :.***.**** :. :*.*  :*:.

EPA505 SRCYHNKLDKQELAAKSVR-VETYKGFIFGCHDPEAPSLEDYLGEFRFYLDTIWEGGGAG 178
CHY-1  SRCYHNKLDKQELAAKSVR-VETYKGFIFGCHDPEAPSLEDYLGEFRFYLDTIWEGGGAG 178
S.y B1 SRCYHNSLDKQKLAAKSVR-VETYKGFIFGCHDPEAPSLEDYLGEFRYYLDTIWEGAGGG 178
S.LH128ERCYHSDLDKSKLGLAPIR-VETYKGFIFGCHDPEAPSLEDYLGDFCWYLDTIWDGPDGG 178
C.A5   EKCYHDELDRDSLSLKTIR-VESYRGFVFGCFDETAPSLEDFLGDWGWYLDTWMVGAGEG 178
S.A4   KELYGGKIDRCAHGLKEVAKVDSYRGFLFGNFDPGAISLEDYLGDVRWYLDIWMEASG-G 175
P.NDO  KDLYGESLNKKCLGLKEVARVESFHGFIYGCFDQEAPPLMDYLGDAAWYLEPMFKHSG-G 179
       .  *  .:::   .   :  *::::**::* .*  * .* *:**:  :**:     . *

EPA505 LELLGPPMKSLLHCNWKVPVENFVGDGYHVGWTHAAALGQIGGLFAGLAGNRADIPFDDL 238
CHY-1  LELLGPPMKSLLHCNWKVPVENFVGDGYHVGWTHAAALGQIGGPLAGLAGNRADIPFDDL 238
S.y B1 MELLGPPMKSLLQCNWKVPAENFIGDGYHVGWTHAAALSQIGGELAGLAGNRADIPFDDL 238
S.LH128LELVGPPLKSTLACNWKVPTENFVGDGYHVGWTHAAALQMIGGELAGLSGNRADMPFDDL 238
C.A5   AELVGPPMKSILKCNWKVPTENFVGDGYHVGWTHASALHVLGGELGGLAGNQAEMPFDEL 238
S.A4   VELIGPPARSIVHCNWKAPTENFVGDAYHIGWTHASSLAASRSIFAPMSGN-QMLPPAGA 234
P.NDO  LELVGPPGKVVIKANWKAPAENFVGDAYHVGWTHASSLRSGESIFSSLAGN-AALPPEGA 238
        **:*** :  : .***.*.***:**.**:*****::*    . :. ::**   :*

EPA505 GLQFTTRHGHGFGLVDNAAAAIHRKG--DGWNKYLEDTRGEVRRKFGADRERLYVGHWNG 296
CHY-1  GLQFTTRHGHGFGVIDNAAAAIHRKG--DGWNKYLEDTRGEVRRKFGADRERLYVGHWNG 296
S.y B1 GLQFTTRHGHGFGVIDNAAAGLHIKR--EGWTKFLEDTRGEVRRKFGPERERLYLGHWNC 296
S.LH128GLQFTMRHGHGFGLIDNAATAIHVKR--DGYVKYLEQTRGGIREKFGPERERLYVGHWNT 296
C.A5   GIQVTTRHGHGFGVIDNAAIAIHAKR--DEYAKYMEETIPKVAENLGEPRAKLFNGHWNC 296
S.A4   GAQIATRFGHGLGILYDVNPGVHTAQTAEKILAWQATKKDKIAEKYGELKARFYGSHLNG 294
P.NDO  GLQMTSKYGSGMGVLWDGYSGVHSADLVPELMAFGGAKQERLNKEIGDVRARIYRSHLNC 298
       * *.: :.* *:*:: :   .:*          :   .   : .: *  : ::: .* *

EPA505 AIFPNCSFLYGTNTFKIWHPRGPHEIEVWTYTMVPSDADPATKSAIQREATRTFGTAGTL 356
CHY-1  AIFPNCSFLYGTNTFKIWHPRGPHEIEVWTYTMVPSDADPATKSAIQREATRTFGTAGTL 356
S.y B1 SIFPNCSFLYGTNTFKIWHPRGPHEIEVWTYTIVPRDADPATKSMIQREAIRTFGTAGTL 356
S.LH128SIFPNCSFLYGTNTFKIWHPRGPHEIEVWTYTMVPKNADTETKRSIQREAIRSFGTAGTL 356
C.A5   STFPNCSFLYGTNIFKVWHPRGPHEIEVWSWVIVHKDMSDEGKREVVKQAVRSFGTAGTL 356
S.A4   SLFPNVSYLWGTNTLKIWQPRGPSETEVWTWAMAEKDMPEDLKRDIYNGLHGGFGTAGYW 354
P.NDO  TVFPNNSMLTCSGVFKVWNPIDANTTEVWTYAIVEKDMPEDLKRRLADSVQRTFGPAGFW 358
       : *** * *  :. :*:*:* ..   ***::.:.  :     *  :       **.**
```

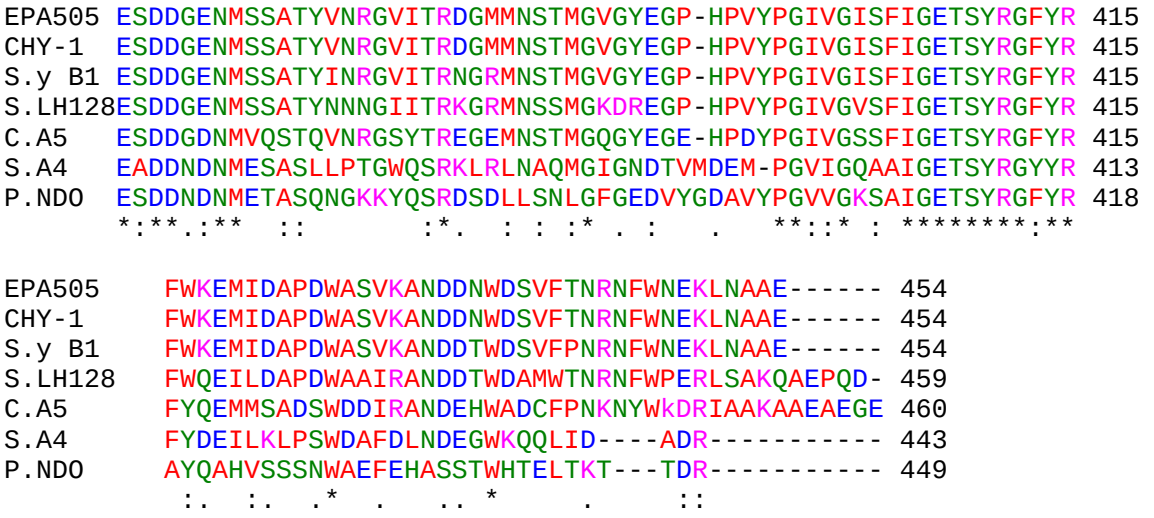

Fig 3.20 Multiple sequence alignment of PhnA1a (alpha subunit of the terminal oxygenase component) with the alpha subunits of *Sphingomonas* sp. CHY-1 (CHY-1), *Sphingobium yanoikuyae* B1 (S. y B1), *Sphingomonas* sp. LH128 (S.LH128), *Cycloclasticus* sp. A4, *Sphingomonas* sp. A4, and the naphthalene dioxygenase alpha subunit of *Pseudomonas* . Fully conserved amino acid residues are indicated by an asterisk. Five conserved histidines and two conserved cysteines are highlighted in yellow. The conserved Asp205 is highlighted in gray. Regions highlighted in red are hypothesized to be responsible for the ability to breakdown large substrates (Leu223, Leu226, Ile253 and Ile260 of CHY-1) (52). Alignment was constructed with ClustalW.

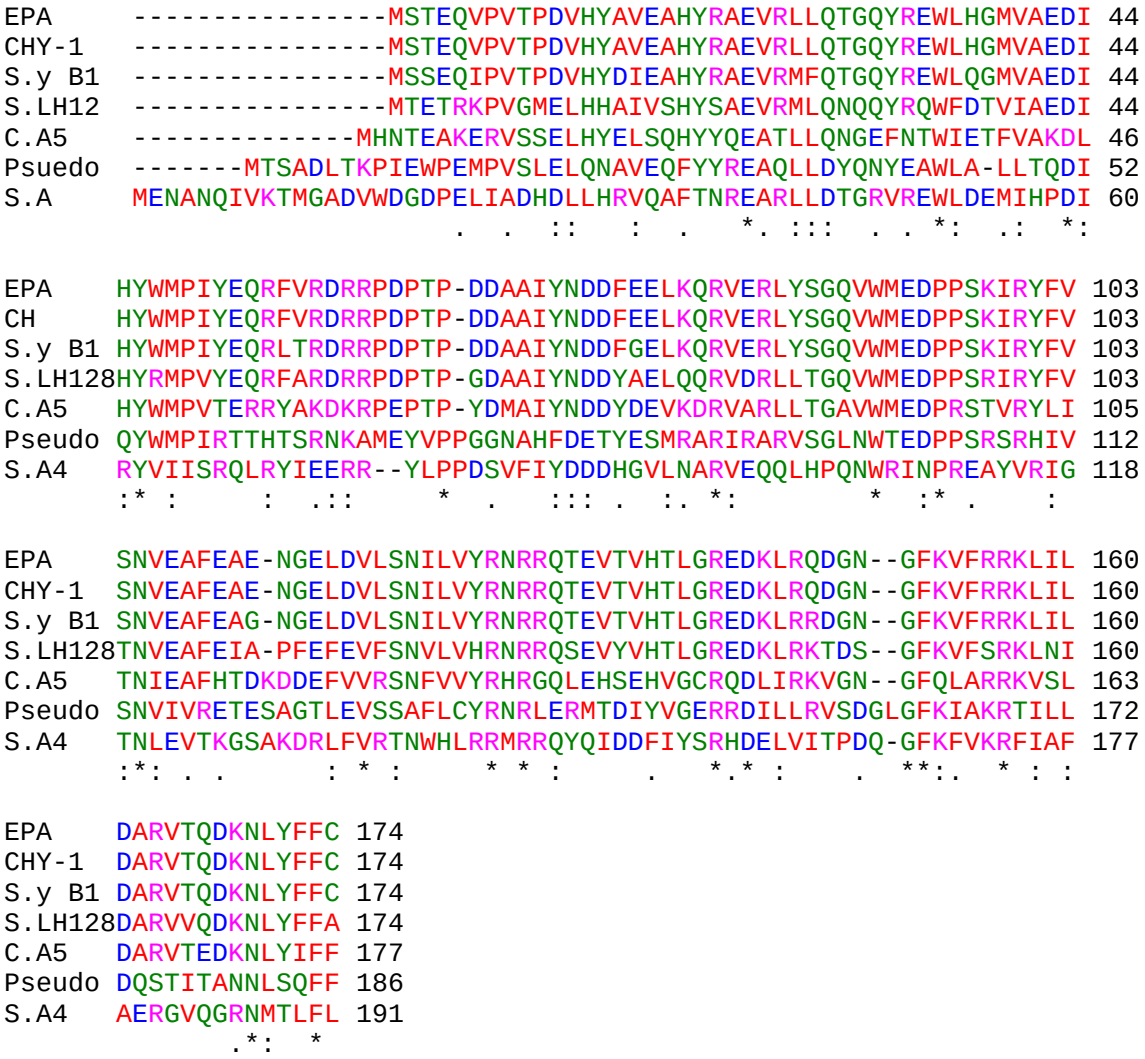

Fig 3.21 Multiple sequence alignment of PhnA2 (beta subunit of the terminal oxygenase component) with the beta subunit of *Sphingomonas* sp. CHY-1 (CHY-1), *Sphingobium yanoikuyae* B1, *Sphingomonas* sp. LH128 (S.LH128), *Cycloclasticus* sp. A5 (C.A5), *Pseudomonas fluorescens*(Pseudo), and *Sphingomonas* sp. A4 (S.A4). Conserved residues are indicated by asterisks.

DISCUSSION

Members of the genus *Sphingomonas* are known for their abilities to breakdown a wider range of PAH substrates compared to other PAH degrading bacteria (40). Because of their potential for bioremediation, it is necessary to study these organisms in more detail to understand the breakdown process at the molecular level. Many enzymes are involved in the PAH breakdown process. The first enzyme in the pathway is always a ring-hydroxylating dioxygenase (28). Dioxygenases are of particular importance since they initiate the pathway by breaking the aromatic ring of the hydrocarbon. Dioxygenases are multi-component enzymes usually consisting of oxygenase components and a ferredoxin and/or a ferredoxin reductase (41).

Sphingomonas paucimobilis EPA505 was isolated from a seven member community at a creosote waste site (34). This organism was able to degrade high molecular weight PAHs and even demonstrated an ability to use one PAH as a sole carbon source. After constructing a BAC library, oligonucleotide probes were designed specifically to target dioxygenase genes. After selecting BAC clones that hybridized to the probe, a shotgun library was constructed to carry out high throughput sequencing.

Sequencing shotgun clones revealed many putative genes (Table 3.1). From the sequencing data assembled, *S. paucimobilis* EPA505 appears to have many different dioxygenases. This is not surprising as other Sphingomonads have been shown to have genes encoding more than one dioxygenase.

Multiple dioxygenase genes were identified and *phnA1a*, *phnA2a*, and *phnA3* were chosen for further analysis. These three genes encode three subunits of a dioxygenase. All together these proteins were expected to form a dioxygenase complex which could breakdown both high and low molecular weight PAHs. The three genes encode an alpha and beta oxygenase component, and a ferredoxin component respectively. According to Demaneche et al. (38), a fourth gene encoding a ferredoxin reductase subunit was also necessary for optimal activity. However this gene was not identified in the assembled sequences of this study. Multiple rounds of PCR and sequencing were carried out to eventually obtain the entire sequence of a gene which was 100% similar to the *ahdA4* gene of *Spingomonas* sp. P2. This gene encodes a ferredoxin reductase and was named *phnA4* for this study.

Phylogenetic analysis of the PhnA1a and PhnA2a subunits showed similarity of these terminal oxygenase components to many other naphthalene dioxygenase like enzymes in various organisms (Fig. 3.18 and 3.19). A multiple sequence alignment revealed some amino acid conservation in the beta subunit, but much more conservation among the alpha subunits (Fig. 3.20 and 3.21). All alpha subunits aligned showed five conserved histidine and two conserved cysteine residues which are believed to be critical for protein function. The Asp205 residue was also conserved among all enzymes. This amino acid is thought to directly connect the active iron center of one alpha subunit to the neighboring unit as the main route for electron transfer (58).

All four genes were cloned for expression. BL21(DE3) host cells expressing the oxygenase components only as well as cells expressing all four components were

induced. When BL21(DE3)(pD12) cells harboring the plasmid to express PhnA1a and PhnA2a oxgenase subunits were induced with IPTG, a 53 kD and 21 kD protein was detected by SDS-PAGE (Fig 3.7). These two bands indicated the successful expression of the *phnA1a* and *phnA2a* genes since they were present only in the induced samples.

When BL21(DE3) cells harboring the plasmids pD12 and pACD34 were induced for expression, the only bands detected by SDS-PAGE were representative of the *phnA1a* and *phnA2a* genes of pD12 (Fig 3.9). No expression was seen for either ferredoxin component (*phnA3*, *phnA4*) cloned on the pACD34 plasmid. Unsuccessful expression could be attributed the plasmid copy number. Plasmid pD12 carrying the genes *phnA1a* and *phnA2a*, was derived from pETDuet-1. This vector has an estimated copy number of 40. Plasmid pACD34 carrying the two genes encoding the ferredoxin components, namely *phnA3* and *phnA4*, was derived from pACYCDuet-1. This vector has an estimated copy number of 10. Because the latter has a much lower copy number, and because copy number probably decreases as genes are cloned into the vector, the amount of expression subsequently decreased. This might explain why expression of the genes cloned into the vector with the higher copy number was only visible with SDS-PAGE.

Another explanation could be that there was a problem in the construction of the plasmids for expression. Sequencing was carried out to confirm genes were in frame after cloning. However, to be sure that the lack of expression was not an issue with the vector, pACD34 was introduced into BL21(DE3) cells to check for expression in the absence of pD12. BL21(DE3) cells were also transformed with pACD3 which only harbored the *phnA3* gene. After induction of BL21(DE3)(pACD3), an appropriately

sized band of 15 kD was observed with SDS-PAGE indicating successful expression of PhnA3. After inducing BL21(DE3)(pACD34), a 15 kD band and another band below the 50 kD mark were observed. The band below the 50 kD mark was assumed to be the 45 kD ferredoxin reductase component as it was only present in the induced samples. In addition, the 15 kD size band representing the *phnA3* gene product was lower in concentration compared to when this gene was expressed alone. This was another indication that both genes were being expressed.

The successful expression of the *phnA3* and *phnA4* genes in the absence of pD12 confirmed that there was no problem with the expression vector or the construct. The lack of expression seen was probably due to the low copy number. When cells harboring both plasmids are induced to express all four subunits, the ferredoxin components were most likely being expressed. However, expression was at such a low level that these proteins were not being detected by SDS-PAGE.

Enzyme activity of the recombinant proteins was examined. To look for dioxygenase activity, BL21(DE3)(pACD34) and BL21(DE3)(pD12) cells were both tested for the ability to transform PAHs into their corresponding dihydrodiol products.

Demaneche et al. observed enzyme activity, albeit minimal, when the oxygenase components of *Sphingomonas* CHY-1 were expressed in the presence of PAHs. When cells expressing only the PhnA1a and PhnA2a proteins of CHY-1 were incubated with various PAHs, dihydrodiol products were detected (38). Although the activity was much lower than the activity observed by cells carrying all four subunits, the two oxygenase components were able to transform the PAHs without the ferredoxin components. To test

this for EPA505's dioxygenase, BL21(DE3)(pD12) cells harboring the plasmid to express only the PhnA1a and PhnA2a products were grown in the presence of PAHs. However, unlike experiments with CHY-1, no dihydrodiol product was detected by GC-MS.

When BL21(DE3)(pD12)(pACD34) was incubated with naphthalene, a product with the GC-MS characteristics of a naphthalene dihydrodiol was detected. The EI mass spectrum of this product was compared to the previously described mass spectra of naphthalene dihydrodiol formed by *Mycobacterium vanbaalenii* (45). The similarities between the mass spectra obtained in this study and that of Kim et al. (45) confirmed the presence of naphthalene dihydrodiol.

When cells expressing the complete dioxygenase were incubated with phenanthrene, the presence of a phenanthrene dihydrodiol was confirmed by comparing the mass spectra obtained to that of Kim et al. (45). The fragmentation patterns observed for the products detected confirm the presence of dihydrodiols. These dihydrodiols are evidence of dioxygenase activity and show the ability of these recombinant proteins to work together to transform the PAH substrates into corresponding breakdown products.

BL21(DE3)(pD12)(pACD34) cells expressing all four subunits of the dioxygenase were able to break down naphthalene and phenanthrene into corresponding dihydrodiols, whereas cells expressing only the oxygenase components showed no dioxygenase activity. The difference in activity supports the idea that the ferredoxin components were being expressed even though they were not detected by SDS-PAGE.

It appears that in EPA505, all four components are necessary for dioxygenase activity. However, the enzyme activity is being analyzed with recombinant proteins. This might have an effect on the stability of the proteins in the cell, as compared to when they are produced naturally by EPA505. Considering the similarity between the *phnA1a* and *phnA2a* genes of EPA505 and those in *Sphingomonas* CHY-1, it is difficult to believe that their protein products do not have some ability to transform PAHs without the ferredoxin components. It is also possible that some of the other dioxygenases identified may show PAH degrading activity without the ferredoxin components. Until all factors are taken into account, and all assay conditions are tested, it cannot be said with certainty that all four components are absolutely required for activity.

When the enzyme was exposed to the HMW PAH, fluoranthene, no breakdown products were observed in the whole cell assay or the assay using cell lysate. The lack of activity with the whole cell assay could be attributed to an inability of the BL21(DE3) cells to take up the fluoranthene. This host does not secrete overexpressed proteins into the media. Therefore, the only way for the proteins and the substrate to interact would be for the substrate to enter the cell. When the whole cell assay was carried out for naphthalene and phenanthrene, dihydrodiol products were identified. More importantly, there was little or none of the original substrate in the supernatant of the cells expressing the enzyme as well as the control cells. The lack of the original substrate, even in the control cells where no breakdown products were detected, is probably an indication that the PAH is entering the cell where it can come in contact with the enzyme. With the fluoranthene experiments, however, no dihydrodiol products were identified and unlike

the other substrates, fluoranthene remained in the supernatant. Since fluoranthene is a larger compound than naphthalene and phenanthrene, it is possible that this substrate is not entering the cell as easily and is not coming in contact with the enzyme. This may be one reason why fluoranthene was not broken down as expected.

To ensure contact between the enzyme and fluoranthene, another activity assay was carried out using the cell lysate. Once again, no dihydrodiol products were identified. However, the lack of activity against fluoranthene does not rule out the ability of this enzyme to break down HMW PAHs. Even though fluoranthene was not broken down, this could be due to instability on the part of the enzyme. After induction, cells were resuspended in a simple Tris buffer and lysed. This lysate was then used to test activity against fluoranthene. It is possible that the buffering conditions were not optimal and the recombinant proteins were not stable after cell lysis. If this assay is repeated, the cell lysate should also be tested against naphthalene and phenanthrene as controls since the enzyme was shown to degrade these compounds.

There is a possibility that the substrate range of the PhnI protein in EPA505 is just not the same as other dioxygenases. BLAST similarity search results indicate the terminal oxygenase components of EPA505 are 99% similar to those of *Sphingomonas* CHY-1. However, CHY-1 was shown to have great versatility in breaking down both low and high molecular weight PAHs. When the crystal structure of the PAH degrading dioxygenase of CHY-1 was determined by Jakoncic et al. (52), the authors found that the catalytic pocket of the enzyme from CHY-1 is at least 2Å longer, wider and higher at the entrance when compared to other ring-hydroxylating dioxygenases. This larger pocket

was attributed to the amino acids Leu_{223}, Leu_{226}, Ile_{253}, and Ile_{260}. The multiple sequence alignment indicates that EPA505's alpha subunit only contains the Leu_{226} and the Ile_{260}. This may be a reason why EPA505 was unable to breakdown fluoranthene. Although PhnA1a of EPA505 shares such high similarity with the PhnA1 of CHY-1, the differences in these amino acid residues may account for EPA505's inability to breakdown larger substrates.

Sphingomonas paucimobilis EPA505 has great potential as a tool for bioremediation. In this study, a multi-component dioxygenase was identified and tested for activity against different PAHs. To our knowledge this is the first report of functional analysis of dioxygenase from EPA505. Future studies will include a more detailed analysis of this enzyme as well as the other dioxygenases identified. Testing enzyme activity in different environments in order to find out optimal activity conditions as well as conditions which inhibit activity may eventually lead to better bioremediation strategies.

REFERENCES

1. Ye, D., *et al*. 1996. Degradation of polynuclear aromatic hydrocarbons by *Sphingomonas paucimobilis*. *Environ. Sci. Technol*. 30:136-42.
2. Krivobok, S., *et al*. 2003. Identification of pyrene-induced proteins in *Mycobacterium* sp. Strain 6PY1: Evidence for two ring-hydroxylating dioxygenases. *J. Bacteriol*. 185:3828-41.
3. Spriggs, T., *et al*. 2005. Phytoremediation of Polycyclic Aromatic Hydrocarbons in Manufactured Gas Plant-Impacted Soil. *J. Environ. Qual*. 34:1755-62.
4. Bouchez, M., *et al*. 1995. Substrate availability in phenanthrene biodegradation: Transfer mechanism and influence on metabolism. *Appl. Microbiol. Biotechnol.* 43:952-960.
5. Kusk, K.O. 1981. Effects of naphthalene on the diatom *Phaeodactylum tricornutum* grown under varied conditions. *Bot. Mar*. 24:485–487.
6. Pipe, R.K., and Moore, M.N. 1986. Arylsulphatase activity associated with phenanthrene induced digestive cell deletion in the marine mussel *Mytilus edulis*. *J. Histochem*. 18:557–564.
7. Passino-Reader, D.R., *et al*. 1995. Chronic bioassays of rainbow trout fry with compounds representative of contaminants in Great Lakes fish. *J. Great Lakes Res.* 21:373–383.
8. Savino, J.F., and Tanabe, L.L. 1989. Sublethal effects of phenanthrene, nicotine, and pinane on *Daphniz pulex*. *Bull. Environ. Contam. Toxicol*. 42:778-784.

9. Cerniglia, C.E. 1984. Microbial metabolism of polycyclic aromatic hydrocarbons. *Adv. Appl. Microbiol.* 30:31-71
10. Geiselbrecht, A.D., *et al*. 1998. Isolation of marine polycyclic aromatic hydrocarbon (PAH)-degrading *Cycloclasticus* strains from the Gulf of Mexico and comparison of their PAH degradation ability with that of Puget Sound *Cycloclasticus* strains. *Appl. Environ. Microbiol*. 64: 4703-10.
11. Agency for Toxic Substances and Disease Registry. 1996. ToxFAQs for Polycyclic Aromatic Hydrocarbons (PAHs). Retrieved September 10, 2010, from http://www.atsdr.cdc.gov/tfacts69.html.
12. Falahatpisheh, M.H., *et al*. 2001. Antagonistic interactions among nephrotoxic polycyclic aromatic hydrocarbons. *J. Toxicol. Environ. Health*. 62:543-560
13. Mastrangela, G. *et al*. 1997. Polycyclic aromatic hydrocarbons and cancer in man. *Environ. Health Perspect*. 104:1166-1170.
14. Cerniglia, C. E. 1992. Biodegradation of polycyclic aromatic hydrocarbons. *Biodegradation*. 3:351–368.
15. Carls, M.G., *et al*. 2004. Pink salmon spawning habitat is recovering a decade after the Exxon Valdez oil spill. *Trans. Amer. Fish. Soc.* 133:834-44.
16. Christen, K. 2003. High PAH levels in dust from 9-11 disaster. *Environ. Sci. Technol.* 37:49A-50A.
17. Hammel, K.E. *et al*. 1986. Oxidation of polycyclic aromatic hydrocarbons and dibenzo[p]-dioxins by *Phanerochaete chrysosporium* ligninase. *J. Biol. Chem*. 261:16948-52.

18. Bezalel, L., *et al*. 1996. Metabolism of phenanthrene by the white rot fungus *Pleurotus ostreatus*. *Appl. Environ. Microbiol.* 62:2547-2553

19. Heitkamp, M.A. and Cerniglia, C.E. 1988. Mineralization of polycyclic aromatic hydrocarbons by a bacterium isolated from sediment below an oil field. *Appl. Environ. Microbiol*. 54:1612-1614.

20. Juhasz, A., *et al*. 1997. Degradation of fluoranthene, pyrene, benz[a]anthracene and dibenz[a,h]anthracene by *Burkholderia cepacia*. *J. Appl. Microbiol*. 83:189-98.

21. Weissenfels, W.D., *et al*. 1991. Microbial metabolism of fluoranthene; isolation and identification of ring fission products. *Appl. Microbiol. Biotechnol*. 34:677-94.

22. Shuttleworth, K. L., and Cerniglia, C.E.. 1995. Environmental aspects of PAH biodegradation. *Biochem. Appl. Biotechnol*. 54:291–302.

23. Bucker, M., *et al*. 1979. Mutagenicity of phenanthrene and phenanthrene K-region derivatives. *Mutat. Res.* 66:337–348.

24. McConkey, B.J., *et al*. 1997. Toxicity of a PAH photooxidation product to the bacteria *Photobacterium phosphoreum* and the duckweed *Lemna gibba*: Effects of phenanthrene and its primary photoproduct, phenanthrenequinone. *Environ. Toxicol. Chem*. 16:892–899.

25. Holt, J., *et al*. 2005. 9,10-Phenanthrenequinone photoautocatalyzes its formation from phenanthrene, and inhibits biodegradation of naphthalene. *J. Environ. Qual*. 34:462-8.

26. Lantz, S.E., *et al*. 1997. Constituents of an organic wood preservative that inhibit the fluoranthene-degrading activity of *Sphingomonas paucimobilis* strain EPA505. *Environ. Sci. Technol*. 31:3573-80.

27. Balkwill, D.L., *et al*. 2006. *Sphingomonas* and related genera. *Prokaryotes*. 7:605-629.

28. Omori, T. and Habe, H. 2003. Genetics of polycyclic aromatic hydrocarbon metabolism in diverse aerobic bacteria. *Biosci. Biotechnol. Biochem*. 67:225-243.

29. Fredrickson, J.K. *et al*. 1991. Isolation and characterization of a subsurface bacterium capable of growth on toluene, naphthalene, and other aromatic compounds. *Appl. Environ. Microbiol*. 57:796-803.

30. Fredrickson, J. K. *et al*. 1995. Aromatic degrading *Sphingomonas* isolates from the deep subsurface. *Appl. Environ. Microbiol*. 61:1917-1922.

31. Zylstra G.J. and Kim, E. 1997. Aromatic hydrocarbon degradation by *Sphingomonas yanoikuyae* B1. *J. Indian Microbiol. Biotechnol*. 19:408-414.

32. Story, S. 2000. Delineation of catabolic pathways for utilization of polycyclic aromatic hydrocarbons by *Sphingomonas paucimobilis* EPA505. Dissertation. Clemson University.

33. Mueller, J. G., *et al*. 1989. Action of a fluoranthene-utilizing bacterial community on polycyclic aromatic hydrocarbon components of creosote. *Appl. Environ. Microbiol*. 55:3085–3090.

34. Mueller, J. G., *et al*. 1990. Isolation and characterization of a fluoranthene-utilizing strain of *Pseudomonas paucimobilis*. *Appl. Environ. Microbiol*. 56:1079–1086.

35. Zylstra, G.J. *et al.* 1997. Comparative molecular analysis of genes for polycyclic aromatic hydrocarbon degradation. *Genet. Eng*. 19:257-269

36. Romine, M.F. *et al*. 1999. Complete sequence of a 184-kilobase catabolic plasmid from *Sphingomonas aromaticivorans* F199. *J. Bacteriol*. 181:1585-1602.

37. Pinyakong, O. *et al*. 2003 The unique aromatic catabolic genes in *Sphingomonads* degrading polycyclic aromatic hydrocarbons (PAHs). *J. Gen. Appl. Microbiol*. 49:1-19.

38. Demaneche S., *et al*. 2004. Identification and functional analysis of two aromatic ring-hydroxylating dioxygenases from a *Sphingomonas* strain that degrades various polycyclic aromatic hydrocarbons. *Appl. Environ. Microbiol.* 70:6714-6725.

39. Kanaly, R.A., and Harayama, S. 2000. Biodegradation of high-molecular-weight polycyclic aromatic hydrocarbons by bacteria. *J. Bacteriol*. 182:2059-67.

40. Story, S. P. *et al*. 2000. Identification of four structural genes and two putative promoters necessary for utilization of naphthalene, phenanthrene, and fluoranthene by *Sphingomonas paucimobilis* var. EPA505. *Gene* 260:155-169.

41. Butler, C.S, and Mason, J.R. 1997. Structure-function analysis of the bacterial aromatic ring-hydroxylating dioxygenases. *Adv. Microb. Physiol.* 38:47-76.

42. Parales, R.E. *et al*. 1999. Aspartate 205 in the catalytic domain of naphthalene dioxygenase is essential for activity. *J. Bacteriol*. 181:1831-1837.

43. Sambrook, J.E., and Russell, D.W. 2001. Molecular cloning: a laboratory manual, 3rd ed., Cold Spring Harbor Laboratory Press, Cold Spring Harbor, NY.

44. Gordon D. *et al*. 1998. "Consed: A Graphical Tool for Sequence Finishing". *Genome Research* 8:195–202.

45. Kim, S. *et al*. 2006. Molecular cloning and expression of genes encoding a novel dioxygenase involved in low and high molecular weight polycyclic aromatic hydrocarbon degradation in *Mycobacterium vanbaalenii* PYR-1. *Appl. Environ. Microbiol*. 72:1045-1054

46. Bojes, H.K and Pope, P.G. 2007. Characterization of EPA's 16 priority pollutant polycyclic aromatic hydrocarbons (PAHs) in tank bottom solids and associated contaminated soils at oil exploration and production sites in Texas. *Reg. Tox. Pharm.* 47:288-295

47. Rozen, S. and Skaletsky, H.J. 2000. Primer 3 on the WWW for general users and for biologist programmers *In*: Krawetz S., and Misener S. (eds). *Bioinformatics Methods and Protocols: Methods in Molecular Biology*. Humana Press, Totowa, NJ, 365-386.

48. Altschul S.F. *et al*. 1990. Basic local alignment search tool. *J. Mol. Biol.* 215:403–10.

49. Besemer J., and Borodovsky M. 2005. GeneMark: web software for gene finding in prokaryotes, eukaryotes and viruses. *Nuc. Acids Res.* 33:451-454.

50. Tamura K. *et al*. 2007. MEGA4: Molecular Evolutionary Genetics Analysis (MEGA) software version 4.0. *Mol. Biol. Evol*. 24:1596-1599.

51. Larkin M.A. *et al*. 2007. ClustalW and ClustalX version 2. *Bioinformatics* 3:2947-2948.

52. Jakoncic, J. *et al*. 2007. The crystal structure of the ring-hydroxylating dioxygenase from *Sphingomonas* CHY-1. *FEBS* 274:2470-2481.

53. Meizhong L., and Rod A. Wing. Methods in Molecular Biology, 236: Plant Functional Genomics: Methods and Protocols. Humana Press, Inc., Totowa, NJ

54. Schuler L. *et al*. 2009. Characterization of a ring-hydroxylating dioxygenase from phenanthrene-degrading *Sphingomonas* sp. Strain LH128 able to oxidize benz[a]anthracene. *Appl. Microbiol. Biotechnol*. 83:465-475.

55. Pinyakong, O. *et al*. 2004. Isolation and characterization of genes encoding polycyclic aromatic hydrocarbon dioxygenase from acenaphthalene and acenaphthylene degrading *Sphingomonas* sp. strain A4. *FEMS* 238:297-305.

56. Chadhain, S. *et al*. 2007. Identification, cloning and characterization of a multicomponent biphenyl dioxygenase from *Sphingobium yanoikuyae* B1. *J. Ind. Microbiol. Biotechnol*. 34:605-613.

57. Dong, X. *et al*. 2005. Crystal structure of the terminal oxygenase component of cumene dioxygenase from *Pseudomonas fluorescens* IP01. *J. Bacteriol*. 187:2483-2490.

58. Parales, R. *et al*. 2000. Substrate specificity of naphthalene dioxygenase: effect of specific amino acids at the active site of the enzyme. *J. Bacteriol*. 182:1641-1649.

59. Kasai, Y. *et al*. 2003. Molecular characterization and substrate preference of a polycyclic aromatic hydrocarbon dioxygenase from *Cycloclasticus* sp. strain A5. *Appl. Environ. Microbiol*. 69:6688-6697.

60. Brown, A. 2008. Sequencing, sub-cloning, expression, and purification of 2-hydroxychromeme-2-carboxylate isomerase from *Sphingomonas paucimobilis* EPA505. Thesis. Clemson University.